

000 001 002 003 004 005 006 007 008 009 010 011 012 013 014 015 016 017 018 019 020 021 022 023 024 025 026 027 028 029 030 031 032 033 034 035 036 037 038 039 040 041 042 043 044 045 046 047 048 049 050 051 052 053 COT-MT³: COT-GUIDED META TEST-TIME TRAINING FOR MULTIMODAL REASONING

Anonymous authors

Paper under double-blind review

ABSTRACT

Large Multimodal Models (LMMs) have achieved remarkable results across various tasks, but they still face challenges in complex multimodal reasoning that is typically performed via chain-of-thought (CoT). Recent studies also start to explore the retrieval-augmented few-shot setting to alleviate this problem. However, existing methods still lack tailored retrieval strategy and effective utilization of demonstrations in complex multimodal reasoning scenarios, resulting in limited reasoning improvements. In this paper, we introduce a novel framework, termed **CoT-Guided Meta Test-Time Training (CoT-MT³)**, to enhance LMMs' few-shot multimodal reasoning ability by employing a CoT-guided Weighted Retrieval (CWR) strategy and a Meta Test-Time Training (MT³) paradigm. To provide more relevant demonstrations, CWR employs a retrieval-specific CoT to highlight key information and deep reasoning of the test query for problem-solving. Retrieval is then performed based on the weighted similarity of both the original query and the derived CoT cues. Moreover, to fully leverage retrieved demonstrations, MT³ introduces a context-based meta-learning paradigm by constructing multiple training samples per query with varying context sizes and combinations using few-shot demonstrations. Experiments across three benchmarks show that our CoT-MT³ achieves a significant relative improvement of up to 4.82% on MathVerse and 8.38% on We-Math in the 4-shot setting. Notably, we observe that our CoT-MT³ demonstrates exceptional robustness across different context sizes, highlighting its effectiveness and generalization to few-shot reasoning scenarios.

1 INTRODUCTION

Large Multimodal Models (LMMs) (Wang et al., 2024b; Liu et al., 2024; Li et al., 2024a) have achieved notable advances in recent years across a wide range of domains. However, they still struggle in solving out-of-distribution questions (Zhang et al., 2024c; Han et al., 2023), especially in complex multimodal reasoning (Zhang et al., 2024a; Wang et al., 2024a) that is typically performed via chain-of-thought (CoT). To alleviate this issue, recent studies (Wang et al., 2023; Zuo et al., 2025; Muennighoff et al., 2025; Snell et al., 2024b; Akyürek et al., 2024) explore test-time scaling strategies, which improves model performance by incorporating additional inference-time compute or task-specific information during inference. Among these strategies, retrieval-augmented methods (Dong et al., 2024; Hübotter et al., 2024) have emerged as a promising direction, which retrieve few-shot demonstrations (also including CoT) at test time to boost the performance of LMMs.

However, these retrieval-augmented approaches remain underexplored in complex reasoning scenarios, which still fall short in achieving accurate retrieval and fully leveraging the retrieved few-shot demonstrations, thus yielding limited improvements. Firstly, existing retrieval mechanisms (Liu et al., 2023; Dong et al., 2024; Tan et al., 2024) primarily rely on question-based similarity between the test query and candidate questions, while overlooking the deep reasoning behind the test query (i.e, the relevant mathematical principles and possible solution strategies). As shown in Figure 1, retrieval solely based on the question leads to the selection of reasoning-level inconsistent demonstrations, and thus fails to provide sufficient support for problem solving. This bias significantly hinders performance on tasks demanding complex multi-step reasoning (Fu et al., 2022).

Furthermore, the complexity of multimodal data also poses significant challenges in leveraging the retrieved few-shot demonstrations. There are two main strategies to leverage these demonstrations:

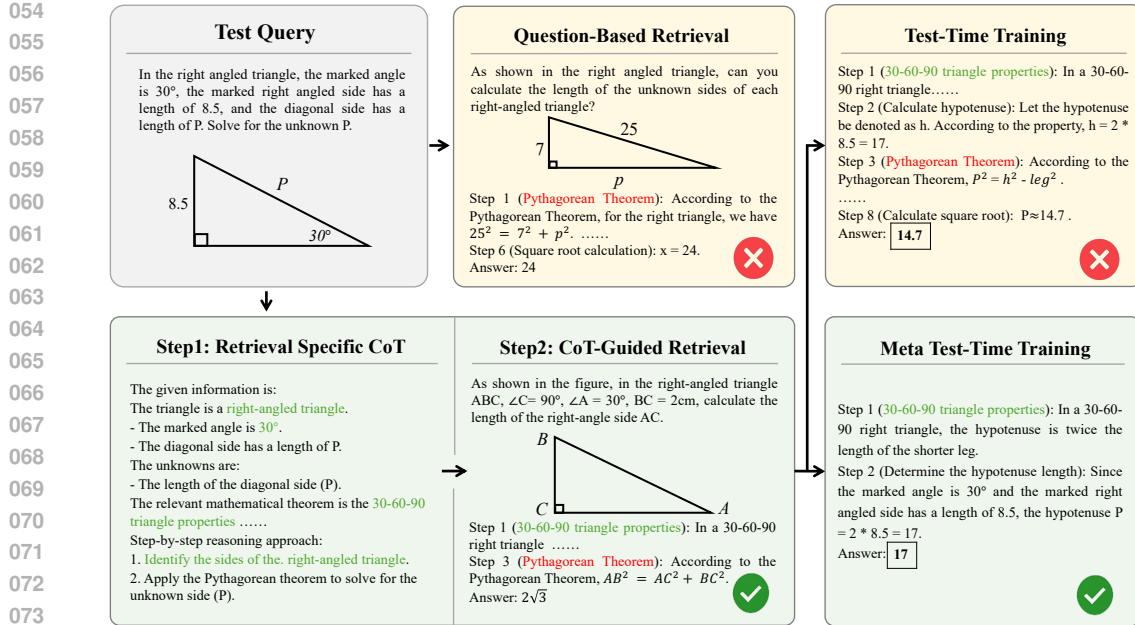


Figure 1: Comparison between different retrieval strategies and training paradigms. It can be seen that CoT-guided retrieval can more effectively search demonstrations with higher similarity in both problem formulation and problem-solving approaches than question-based retrieval. Moreover, simple fine-tuning approach tends to overfit to the retrieval demonstration and copy their reasoning patterns directly, which otherwise can be alleviated by meta test-time training.

1) In-Context Learning (ICL) that provides demonstrations in prompts for reference (Liu et al., 2023; Dong et al., 2024; Tan et al., 2024; Jiang et al., 2024; Qin et al., 2023), and 2) Test-Time Training (TTT) that fine-tunes the model with these lightweight demonstrations at test time (Hardt & Sun, 2024; Hübotter et al., 2024). However, ICL methods struggle to understand complex multimodal prompts with multiple interleaved images and texts. As the number of demonstrations increases, ICL methods even actually harm the reasoning performance (Qin et al., 2024; Liu et al., 2023). Meanwhile, TTT methods tend to overfit to the limited number of demonstrations, causing the model to copy the pattern of the demonstration directly, which leads to incorrect answers (Hübotter et al., 2024). Overall, both groups of retrieval-augmented approaches (i.e., ICL and TTT) fail to fully leverage the retrieved few-shot demonstrations in boosting the reasoning ability of LMMs.

To address the above limitations, we propose a novel framework, termed **CoT-Guided Meta Test-Time Training (CoT-MT³)**, to enhance LMMs’ complex multimodal reasoning performance during test time. The proposed framework consists of two key components: a CoT-guided Weighted Retrieval (**CWR**) strategy and a Meta Test-Time Training (**MT³**) paradigm. As shown in Figure 1, the CWR strategy improves retrieval accuracy through two modules: retrieval-specific CoT and CoT-integrated weighted retrieval. The retrieval-specific CoT decomposes the reasoning process into multiple predefined sub-tasks, guiding the original LMM to highlight key problem information and task-specific knowledge for solving problems, such as relevant mathematical theorems, as illustrated by the green text on the left side of Figure 1. The CoT-integrated weighted retrieval strategy then selects target demonstrations based on the weighted score of question similarity and reasoning similarity (computed between the CoT output and the derived CoT cues).

Built upon CWR, our **MT³** paradigm introduces a context-based meta-learning paradigm designed to improve LMMs’ reasoning ability at test time. Rather than directly fine-tuning on the fixed set of retrieved demonstrations, **MT³** constructs a series of few-shot training samples with varying context sizes and diverse combinations. Each demonstration is treated as the target in turn, while the remaining demonstrations are selected, mixed up and utilized to form its prompt context. This training process encourages the model to learn how to recognize useful information under diverse multimodal prompt conditions. In this way, our method fully leverages the potential of the retrieved demonstrations in mete-learning way to achieve robust reasoning of LMMs at test time.

108 Our contributions are summarized as follows: **1)** We propose CoT-Guided Weighted Retrieval
 109 (CWR) strategy that combines retrieval-specific CoT with a CoT-integrated weighted mechanism to
 110 retrieve demonstrations with higher accuracy. **2)** We introduce MT³, a context-based meta-learning
 111 paradigm that improves the model’s robustness across varying few-shot settings and facilitates effec-
 112 tive reasoning at test time. **3)** Extensive experiments show that the proposed CoT-MT³ significantly
 113 improves LMMs’ complex reasoning ability, and outperforms other competing methods across most
 114 settings, demonstrating its effectiveness in retrieval-augmented reasoning scenarios.

115 2 RELATED WORK

116 **Multimodal Reasoning.** With the growing attention on multimodal reasoning, a variety of meth-
 117 ods (Peng et al., 2024; Shi et al., 2024; Gao et al., 2023) and benchmarks (Zhang et al., 2024a;
 118 Lu et al., 2024; Qiao et al., 2024; Wang et al., 2024a; 2025a) have been introduced, contributing
 119 to advancements in the field. Most existing approaches (Shi et al., 2024; Li et al., 2024b) rely on
 120 fine-tuning LMMs using large-scale multimodal datasets to enhance their reasoning abilities. Due
 121 to the scarcity of high-quality multimodal data, fine-tuning on synthetic data (Zhang et al., 2024b;
 122 Gao et al., 2023) has emerged as a widely adopted strategy, yielding some improvements in model
 123 performance. Recently, test-time scaling techniques have gained traction as an alternative approach
 124 to enhance reasoning performance (Muennighoff et al., 2025; Guan et al., 2025; Ye et al., 2025;
 125 Snell et al., 2024a; Dong et al., 2024). Among them, retrieval-augmented approaches have demon-
 126 strated effectiveness (Dong et al., 2024; Liu et al., 2023; Tan et al., 2024). However, their appli-
 127 cation in complex multimodal reasoning remains largely unexplored. Developing techniques that
 128 can effectively leverage retrieved few-shot demonstrations and adapt LMMs to complex multimodal
 129 reasoning tasks during inference remains a critical challenge.

130 **Test-Time Training.** Test-Time Training (TTT) (Sun et al., 2020; Hardt & Sun, 2024) is a general
 131 approach for enhancing model performance when training and test data come from different distri-
 132 butions. Recent works on TTT have extended this paradigm to LLMs (Hardt & Sun, 2024; Akyürek
 133 et al., 2024; Wang et al., 2024c; Hübotter et al., 2024) by fine-tuning on retrieved demonstrations,
 134 demonstrating its effectiveness on novel tasks. TTT-NN (Hardt & Sun, 2024) improves language
 135 modeling task performance by fine-tuning top- N nearest neighbors retrieved from each test query.
 136 Similarly, TTT-ICL (Akyürek et al., 2024) constructs context-based demonstrations according to
 137 few-shot data for fine-tuning, achieving strong results on the ARC Challenge. However, TTT hasn’t
 138 been explored in complex multimodal reasoning scenarios, particularly in terms of demonstration
 139 multimodal retrieval and effectively reasoning under few-shot conditions.

140 **Chain-of-Thought Reasoning.** Chain-of-Thought (CoT) (Wang et al., 2025b; Wei et al., 2022;
 141 Chen et al., 2025) has significantly advanced LMMs’ reasoning abilities, leading to notable progress
 142 in solving multi-step reasoning tasks. Apart from fine-tuning approaches, existing works explicitly
 143 generate intermediate steps or decompose the problem into manageable subproblems, thereby en-
 144 abling models to tackle complex tasks in a interpretable manner (Zhang et al., 2023; Zheng et al.,
 145 2023; Sun et al., 2025). Recent works (Qin et al., 2023; Trivedi et al., 2022) also propose to leverage
 146 the model’s initial CoT outputs to retrieve relevant demonstrations and enhance downstream tasks
 147 through retrieval-augmented methods. However, these methods overlook the explicit optimization
 148 of the CoT reasoning process for retrieval purpose. In this work, we propose a retrieval-specific CoT
 149 that highlights key information to support tailored demonstration retrieval.

150 3 METHODOLOGY

151 3.1 PRELIMINARY

152 In the retrieval-augmented few-shot setting, given a test query $q_t = \{i_q, t_q\}$, where i_q denotes the
 153 image and t_q denotes the question text, along with a demonstration pool D , the first step is to retrieve
 154 the most relevant m demonstrations from D . This is achieved via a similarity function $S(x_q, x)$ that
 155 ranks each candidate $x \in D$ based on its relevance to the test query x_q :

$$156 \quad X = \{x_1, x_2, \dots, x_m\} = \text{top-}m(D, S(x_q, \cdot)), \quad (1)$$

157 where each retrieved demonstration $x_i = \{q_i, r_i\}$ consists of a question q_i and a corresponding
 158 response r_i , and the function $\text{top-}m(D, S)$ denotes the most relevant m demonstrations from D
 159 according to the similarity function $S(x_q, \cdot)$.

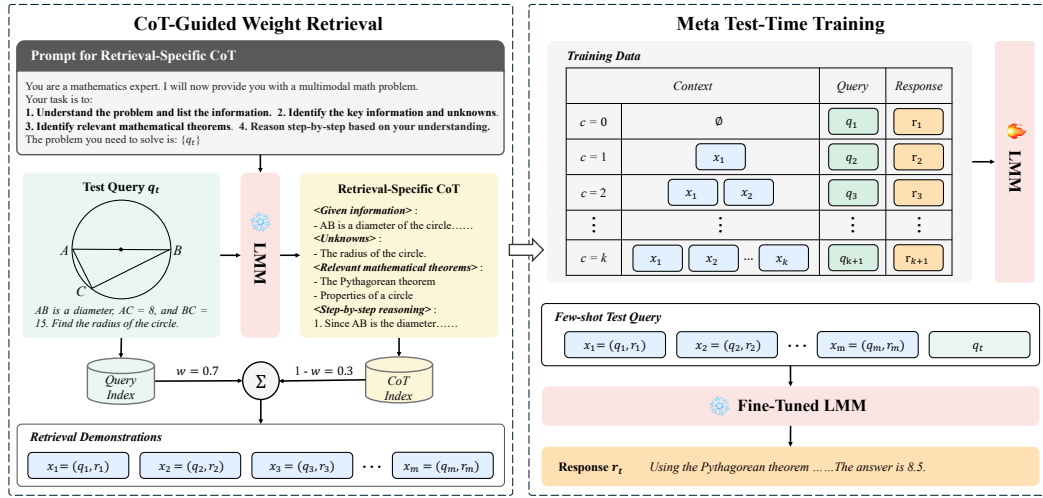


Figure 2: **Overview architecture of our proposed CoT-MT³**. It consists of two novel components: **(1) CoT-Guided Weight Retrieval**: Given the test query q_t , the original LMM first generates a retrieval-specific CoT that captures task-specific information. This information combined with the test query is utilized in a weighted retrieval mechanism to retrieve top- m relevant demonstrations. **(2) Meta Test-Time Training**: Built upon the retrieval demonstrations $\{x_1, x_2, \dots, x_m\}$, the model is fine-tuned using a series of few-shot training samples. For each query with question q_i , multiple training samples ranging from 0-shot to k -shot are constructed by random sampling different subsets of the retrieved demonstrations. During inference, the fine-tuned LMM leverages the test query with k -shot retrieved demonstrations to obtain the final response r_t .

The objective of retrieval-augmented few-shot learning is to: (1) optimize the selection of relevant demonstrations and (2) maximize the model’s ability to generate accurate predictions conditioned on the selected demonstrations. This can be formulated as:

$$\max_{X \subset D} P(r_q | x_q, X), \quad (2)$$

where $P(r_q | x_q, X)$ denotes the probability of generating the response r_q for the query x_q , conditioned on the retrieved demonstrations X .

3.2 OVERALL ARCHITECTURE

Our goal is to enhance LMMs’ reasoning performance under retrieval-augmented few-shot setting. As illustrated in Figure 2, the proposed framework comprises two key components: CoT-guided Weighted Retrieval (CWR) and Meta Test-Time Training (MT³). CWR improves retrieval quality by employing a retrieval-specific CoT that decomposes the initial reasoning process into multiple sub-tasks, guiding the model to highlight key information and task-specific knowledge. A CoT-integrated weighted retrieval mechanism is then employed to select demonstrations by combining question-based similarity and reasoning-based similarity. In the test-time training stage, we propose MT³, a context-based meta-learning paradigm to improve LMMs’ reasoning ability at test time. Rather than simple fine-tuning, MT³ constructs few-shot training samples with varying context sizes and combinations, encouraging the model to learn how to recognize valuable information and achieve effective reasoning from multimodal context. We describe the details of each module below.

3.3 CoT-GUIDED WEIGHTED RETRIEVAL

3.3.1 RETRIEVAL-SPECIFIC CoT

In multimodal reasoning tasks, retrieving highly relevant demonstrations requires precise understanding and deep analysis of the problem content. A natural solution is to leverage the model’s preliminary Chain-of-Thought (CoT) reasoning output as auxiliary information to improve the retrieval precision (Dong et al., 2024; Qin et al., 2023). However, basic CoT prompting strategies (e.g., “Let’s think step by step”) focus solely on solving the target problem, making it difficult to extract the key reasoning information for effective retrieval. The mismatch between CoT objectives

216 and retrieval-specific reasoning demands causes basic CoT prompting to fall short in addressing
 217 retrieval-specific requirements.
 218

219 To address this issue, we propose a retrieval-
 220 specific CoT, which structures the model’s ini-
 221 tial reasoning into a sequence of predefined sub-
 222 tasks aimed at uncovering the deep reasoning be-
 223 hind the test query. As illustrated in Figure 3,
 224 retrieval-specific CoT decomposes the reasoning
 225 into four key stages: understanding and listing the
 226 problem statement, identifying key information
 227 and unknowns, identifying relevant mathemati-
 228 cal theorems, and performing step-by-step rea-
 229 soning based on above understanding. This struc-
 230 tured approach simplifies reasoning by breaking
 231 the problem into manageable components while
 232 highlighting retrieval-critical elements.
 233

234 In contrast to basic CoT prompting which pri-
 235 marily generates calculations steps to reach the
 236 final answer, our approach emphasizes both the
 237 model’s understanding and reasoning patterns of
 238 the problem. By explicitly guiding the model to
 239 construct a retrieval-specific representation of the problem, retrieval-specific CoT ultimately im-
 240 proves the retrieval precision. Moreover, the structure of retrieval-specific CoT can be flexibly
 241 adapted to other domains (e.g., physics) to better capture domain-specific knowledge.
 242

243 3.3.2 CoT-INTEGRATED WEIGHTED RETRIEVAL

244 After obtaining the retrieval-specific CoT output, we aim to incorporate both the question content
 245 and the generated reasoning information into the retrieval process. However, the question’s visual
 246 and textual descriptions already occupy substantial token space, while the generated CoT reasoning
 247 steps tend to be also detailed. As a result, embedding all components into a unified representation
 248 leads to degraded retrieval quality. Furthermore, as different tasks emphasize question and reasoning
 249 to different extents, a task-adaptive weighted mechanism is required to balance their contributions.
 250

251 To this end, we adopt a weighted retrieval strategy that separately computes similarities from ques-
 252 tion and reasoning, and then dynamically adjusts their influence during retrieval. Specifically, given
 253 a test query x_q and the generated retrieval-specific CoT rs_q , we compute two types of similarity:
 254 question-based similarity and reasoning-based similarity. Let $\text{sim}(\cdot, \cdot)$ denote a similarity function.
 255 The question-based similarity s_q is computed between the encoded features of the test query and the
 256 candidate demonstration $x_i = \{i, t_i\}$:
 257

$$258 s_q = \text{sim}(f(x_q), f(x_i)) \quad (3)$$

259 where $f(x_q)$ and $f(x_i)$ denote the joint multimodal feature embedding of the test query and the
 260 candidate demonstration, respectively. The reasoning-based similarity s_r is calculated using the
 261 retrieval-specific CoT output rs_q and the response r_i of the candidate demonstration:
 262

$$263 s_r = \text{sim}(f(rs_q), f(r_i)). \quad (4)$$

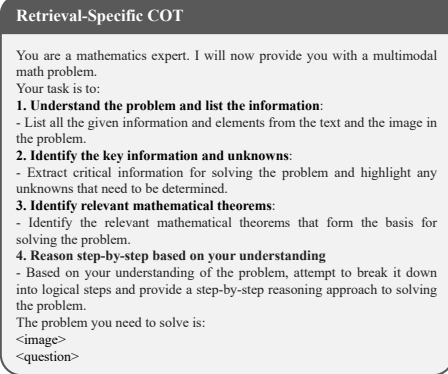
264 To balance their contributions, we define a weighted similarity:
 265

$$266 s = w \cdot s_q + (1 - w) \cdot s_r, \quad (5)$$

267 where $w \in [0, 1]$ is a hyperparameter controlling the trade-off between question-based similarity
 268 and reasoning-based similarity. This weighted design provides fine-grained control over retrieval
 269 relevance, leading to more accurate selection of demonstrations.
 270

271 3.4 META TEST-TIME TRAINING

272 Although retrieval-augmented methods provide relevant demonstrations at test time, effectively util-
 273 izing them to improve multimodal reasoning ability remains challenging. To mitigate this limita-
 274 tion, we propose Meta Test-Time Training (MT³), a context-based meta-learning paradigm. To fully
 275



276 Figure 3: Illustration of retrieval-specific CoT
 277 for multimodal mathematical reasoning, which
 278 decomposes the reasoning process into pre-
 279 defined sub-tasks that guide the model to highlight
 280 task-relevant information.
 281

282

283

284

285

286

287

288

289

290

291

292

293

294

295

296

297

298

299

300

301

302

303

304

305

306

307

308

309

310

311

312

313

314

315

316

317

318

319

320

321

322

323

324

325

326

327

328

329

330

331

332

333

334

335

336

337

338

339

340

341

342

343

344

345

346

347

348

349

350

351

352

353

354

355

356

357

358

359

360

361

362

363

364

365

366

367

368

369

370

371

372

373

374

375

376

377

378

379

380

381

382

383

384

385

386

387

388

389

390

391

392

393

394

395

396

397

398

399

400

401

402

403

404

405

406

407

408

409

410

411

412

413

414

415

416

417

418

419

420

421

422

423

424

425

426

427

428

429

430

431

432

433

434

435

436

437

438

439

440

441

442

443

444

445

446

447

448

449

450

451

452

453

454

455

456

457

458

459

460

461

462

463

464

465

466

467

468

469

470

471

472

473

474

475

476

477

478

479

480

481

482

483

484

485

486

487

488

489

490

491

492

493

494

495

496

497

498

499

500

501

502

503

504

505

506

507

508

509

510

511

512

513

514

515

516

517

518

519

520

521

522

523

524

525

270 leverage the retrieved demonstrations, MT³ fine-tunes the model in a meta-learning paradigm using
 271 a series of few-shot training instances with varying context sizes and combinations. This enables
 272 LMMs to efficiently acquire domain-specific reasoning capabilities at test time, thereby enhancing
 273 the overall performance on complex multimodal reasoning tasks.

274 **Training Set Construction.** As illustrated in Figure 2, we construct a series of few-shot samples for
 275 meta test-time training by varying the number and combination of context demonstrations per query.
 276 Specifically, given the retrieved demonstration set $X = \{x_1, x_2, \dots, x_m\}$, where each $x_i = \{q_i, r_i\}$,
 277 we generate $k+1$ training samples for each target $x_i \in X$. Each sample is assigned a unique context
 278 size from the set $\{0, 1, \dots, k\}$, where $k \leq m-1$ is a predefined maximum context size. For each
 279 context size c , the prompt $P_i^{(c)}$ for target x_i is formed by randomly sampling c demonstrations from
 280 the remaining set:

$$282 \quad \forall x_i \in X, \forall c \in \{0, 1, \dots, k\}, P_i^{(c)} \subset X \setminus \{x_i\}, \quad |P_i^{(c)}| = c. \quad (6)$$

283 Notably, for edge cases such as $c = 0$, there only exist m unique samples. Therefore, we uniformly
 284 sample m training samples for each context size to ensure balanced training across context sizes.
 285 Additionally, we ensure that each demonstration is used equally as both the target and part of the
 286 context, promoting balanced participation and reducing overfitting to specific demonstrations.
 287

288 **Meta Test-Time Training and Inference.** At test time, we adapt the model using pre-constructed
 289 samples generated from retrieved demonstrations. Each training sample consists of a target question
 290 paired with a context with size c . The training objective is defined as:

$$291 \quad \mathcal{L}(x_i, P_i^{(c)}) = -\log P(r_i | q_i, P_i^{(c)}), \quad (7)$$

293 where $P(r_i | q_i, P_i^{(c)})$ denotes the probability of generating the correct response r_i for the target
 294 question q_i , conditioned on its associated context $P_i^{(c)}$. The diversity of multimodal prompt conditions
 295 in the few-shot training samples enables the model to learn how to identify useful information
 296 and enhance reasoning capabilities during meta-training.

297 Final inference is performed by the fine-tuned model. Following Flamingo (Alayrac et al., 2022), we
 298 construct few-shot test query by concatenating original test query and all retrieved demonstrations,
 299 sorted by descending similarity to the test query. The fine-tuned model then performs more accurate
 300 and robust reasoning based on the retrieval-augmented multimodal context.
 301

302 4 EXPERIMENTS

304 4.1 EXPERIMENTAL SETUP

305 **Benchmarks.** We focus on the multimodal mathematical reasoning, which serves as one of most
 306 challenging tasks for multimodal reasoning. Our method is evaluated on three multimodal mathe-
 307 matical reasoning benchmarks: MathVerse (Zhang et al., 2024a), MathVista (Lu et al., 2024), and
 308 We-Math (Qiao et al., 2024), using the testmini sets of each. For MathVerse, we focus on four mul-
 309 timodal subsets: Text Dominant (TD), Text Lite (TL), Vision Dominant (VD), and Vision Intensive
 310 (VI), which all involve both textual and visual inputs. We exclude the Text Only and Vision Only
 311 subsets to ensure that test queries and retrieved demonstrations share the same input modalities. For
 312 MathVista, we evaluate on the Geometric Problem Solving (GPS) subset, and for We-Math, we use
 313 the full set. A more detailed description of these benchmarks is provided in Appendix B.1.

314 **Baselines.** Our method is compared against a range of baseline methods under 2, 4 and 6-shot
 315 settings: (1) **Zero-shot**: direct inference without any demonstrations. (2) **Random**: ICL with ran-
 316 domly sampled demonstrations from the candidate pool. (3) **RICES**: retrieval-based in-context ex-
 317 ample selection (Alayrac et al., 2022), which retrieves demonstrations using visual similarity to the
 318 query. (4) **QBICL**: ICL using question-based retrieval, incorporating both the image and question
 319 text in the similarity computation. (5) **TTT-NN**: TTT on nearest retrieved demonstrations, following
 320 the setup in Hardt & Sun (2024). (6) **TTT-ICL**: TTT using in-context demonstrations, where we
 321 follow the leave-one-out construction strategy in Akyürek et al. (2024). Note that both TTT-NN
 322 and TTT-ICL adopt question-based retrieval to ensure consistency in comparison.

323 **Implementation Details.** For the retrieval component, we employ Vista (Zhou et al., 2024), a
 324 multimodal hybrid retriever capable of processing long input sequences. All retrieval tasks are

324
 325 Table 1: Comparative results on MathVerse under 2-shot, 4-shot, and 6-shot settings. Accuracy (%)
 326 is used as the evaluation metric. The best score for each setting is **bolded**. All compared methods
 327 employ the same backbone Qwen2-VL-7B.

Methods	TD			TL			VI			VD			Avg		
	2-shot	4-shot	6-shot												
Zero-shot	32.49	32.49	32.49	27.41	27.41	27.41	23.73	23.73	23.73	24.49	24.49	24.49	27.03	27.03	27.03
Random	31.35	30.33	31.60	27.03	25.89	25.63	22.59	22.34	25.00	23.22	24.37	25.13	26.05	25.73	26.84
RICES	33.50	36.17	34.39	28.30	29.57	28.55	24.37	26.65	25.76	22.59	22.72	24.62	27.19	28.78	28.33
QBICL	36.80	36.80	37.69	27.92	29.19	27.66	24.49	25.12	25.76	23.98	25.63	23.60	28.30	29.19	28.68
TTT-NN	37.06	38.96	36.80	28.55	29.19	29.19	24.75	24.87	27.03	24.11	26.40	26.40	28.62	29.86	29.86
TTT-ICL	37.06	37.06	38.07	28.93	31.47	27.92	25.00	27.53	25.63	25.76	26.52	23.35	29.19	30.65	28.74
CoT-MT ³	34.77	40.36	39.97	30.46	31.60	33.88	27.28	27.66	27.16	24.87	27.79	27.79	29.35	31.85	32.20

338
 339 Table 2: Comparative results on MathVista (GPS subset) under 2-shot, 4-shot, and 6-shot settings.
 340 Accuracy (%) is used as the evaluation metric. The best score for each setting is **bolded**.

Shots	Zero-shot	Random	RICES	QBICL	TTT-NN	TTT-ICL	CoT-MT ³
2-shot	46.15	42.31	42.31	48.56	49.52	52.40	57.21
4-shot	46.15	40.87	49.04	46.63	54.81	56.25	60.58
6-shot	46.15	39.42	50.96	45.67	55.77	53.37	59.62

346 conducted from the MultiMath-300K (Peng et al., 2024) corpus, a high-quality multimodal bilingual
 347 dataset with detailed CoT annotations. To preserve linguistic consistency and semantic alignment,
 348 we retrieve demonstrations in the corresponding language of the input query. We employ LoRA (Hu
 349 et al., 2022) fine-tuning with a rank of 8 and a scaling factor $\alpha = 16$. The model is optimized using
 350 the Adam (Kingma & Ba, 2014) optimizer with a learning rate of 0.0002 and a weight decay of 0.1.
 351 The w for CWR is set to 0.7 and the k for MT³ is defined as $\lfloor m/2 \rfloor$, where m represents the number
 352 of retrieved demonstrations. All experiments are conducted on 4 NVIDIA A800 GPUs.

354 4.2 MAIN RESULTS

355 4.2.1 RESULTS ON MATHVERSE AND MATHVISTA

356 **Effectiveness of CoT-MT³.** As shown in Tables 1 & 2, our CoT-MT³ consistently achieves the
 357 best or near-best performance across all subsets and few-shot settings. For example, on the TD
 358 subset, our CoT-MT³ outperforms TTT-ICL by 3.30% and zero-shot baseline by up to 7.87% under
 359 the 4-shot setting. Similarly, on the GPS subset, it exceeds TTT-ICL by 4.33% and surpasses zero-
 360 shot baseline by up to 14.43%. Across all 18 evaluation settings ((5 subsets + 1 avg) \times 3 few-shot
 361 settings), our CoT-MT³ achieves the highest score in 16 out of 18 settings (including the average
 362 evaluation settings). These results highlight the strong generalization ability of our CoT-MT³, es-
 363 tablishing it as an effective framework for retrieval-augmented multimodal reasoning.

364 **Potential of TTT-Based Methods.** TTT-based methods exhibit strong potential in retrieval-
 365 augmented reasoning tasks. Among them, TTT-NN that performs direct fine-tuning on retrieved
 366 demonstrations, shows consistent gains as the number of retrieved demonstrations increases. How-
 367 ever, it only employs simple fine-tuning paradigm and thus shows only limited improvement, in
 368 comparison with TTT-ICL and CoT-MT³ which incorporate retrieved demonstrations as context.

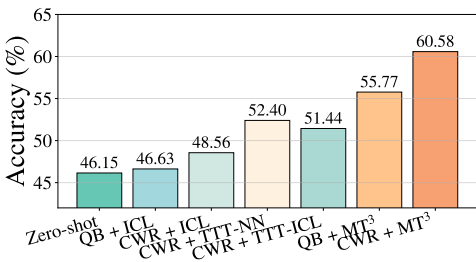
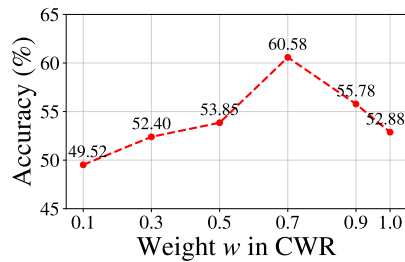
369 Furthermore, although TTT-ICL generally outperforms TTT-NN in the 2- and 4-shot settings, its
 370 performance declines in the 6-shot scenario. This degradation is likely due to a mismatch between
 371 the context length used during training and those encountered at test time. Specifically, the leave-
 372 one-out construction strategy of TTT-ICL treats each retrieved demonstration as a test instance, with
 373 the rest forming its context, leading to shorter training inputs. Such a mismatch may hinder the
 374 model’s adaptation to longer and more complex test-time prompts.

375 In comparison, our proposed CoT-MT³ achieves consistently strong performance across all few-shot
 376 configurations. This robustness can be attributed to its meta-learning paradigm, which enhances the
 377 model’s ability to generalize by adapting to varying multimodal prompt conditions.

378

379
380
381
Table 3: Comparative results on We-Math. Five evaluation metrics are reported: IK (insufficient
knowledge), IG (inadequate generalization), CM (complete mastery), RM (rote memorization), and
Avg (loose overall average scores). The best score for each setting is **bolded**.

Methods	IK (↓)			IG (↓)			CM (↑)			RM (↓)			Avg (↑)		
	2-shot	4-shot	6-shot	2-shot	4-shot	6-shot	2-shot	4-shot	6-shot	2-shot	4-shot	6-shot	2-shot	4-shot	6-shot
Zero-shot	56.19	56.19	56.19	12.95	12.95	12.95	25.14	25.14	25.14	18.52	18.52	18.52	31.62	31.62	31.62
Random	57.90	61.90	57.33	9.90	10.10	11.43	26.86	24.38	25.90	16.57	12.93	17.07	31.81	29.43	31.62
RICES	60.19	58.86	56.00	11.43	9.14	9.71	22.67	26.10	30.48	20.13	18.45	11.11	28.38	30.67	35.33
QBICL	56.76	60.00	55.81	7.81	8.00	10.48	29.33	26.48	27.81	17.20	17.26	17.51	33.24	30.48	33.05
TTT-NN	54.67	53.52	56.76	10.86	12.29	10.67	29.14	29.52	27.62	15.47	13.89	15.20	34.57	35.62	32.95
TTT-ICL	58.29	52.76	55.62	7.62	10.67	8.95	27.62	30.48	31.43	18.99	16.67	11.29	31.43	35.81	35.90
CoT-MT ³	55.81	49.90	53.52	9.14	10.67	8.95	30.48	34.67	32.19	13.04	12.08	14.21	35.05	40.00	36.67

401
402
Figure 4: **Ablation results for different components of CoT-MT³ on MathVista (GPS).**401
402
Figure 5: Ablation results for different w values in the CWR strategy on MathVista (GPS).

403
404
405
406
407
408
409
410
411
Validity of Reasoning Information for Retrieval. RICES relies solely on visual input and per-
forms well in vision-intensive subsets but struggles in text-centric subsets (e.g., MathVerse TD). In
contrast, QBICL considering both textual and visual components, yields more balanced performance
across different subsets, consistent with findings from prior work (Qin et al., 2024). Built on this,
our CoT-MT³ further integrates reasoning information into the retrieval, guiding demonstration se-
lection based not only on question content but also on underlying reasoning semantics. According to
Tables 1 & 2, the reasoning-guided retrieval proves particularly effectiveness for complex multi-step
reasoning problems. Overall, it suggests that progressively enriching the retrieval information (from
visual, to multimodal, to CoT-guided), substantially improves the relevance of demonstrations.

4.2.2 MORE RESULTS ON WE-MATH

412
413
Table 3 presents the evaluation results on We-Math across five diagnostic metrics. Our CoT-MT³
414
415
416
417
418
419
420
421
422
423
424
425
426
427
428
429
430
431
432
433
434
435
436
437
438
439
440
441
442
443
444
445
446
447
448
449
450
451
452
453
454
455
456
457
458
459
460
461
462
463
464
465
466
467
468
469
470
471
472
473
474
475
476
477
478
479
480
481
482
483
484
485
486
487
488
489
490
491
492
493
494
495
496
497
498
499
500
501
502
503
504
505
506
507
508
509
510
511
512
513
514
515
516
517
518
519
520
521
522
523
524
525
526
527
528
529
530
531
532
533
534
535
536
537
538
539
540
541
542
543
544
545
546
547
548
549
550
551
552
553
554
555
556
557
558
559
560
561
562
563
564
565
566
567
568
569
570
571
572
573
574
575
576
577
578
579
580
581
582
583
584
585
586
587
588
589
590
591
592
593
594
595
596
597
598
599
600
601
602
603
604
605
606
607
608
609
610
611
612
613
614
615
616
617
618
619
620
621
622
623
624
625
626
627
628
629
630
631
632
633
634
635
636
637
638
639
640
641
642
643
644
645
646
647
648
649
650
651
652
653
654
655
656
657
658
659
660
661
662
663
664
665
666
667
668
669
670
671
672
673
674
675
676
677
678
679
680
681
682
683
684
685
686
687
688
689
690
691
692
693
694
695
696
697
698
699
700
701
702
703
704
705
706
707
708
709
710
711
712
713
714
715
716
717
718
719
720
721
722
723
724
725
726
727
728
729
730
731
732
733
734
735
736
737
738
739
740
741
742
743
744
745
746
747
748
749
750
751
752
753
754
755
756
757
758
759
7510
7511
7512
7513
7514
7515
7516
7517
7518
7519
7520
7521
7522
7523
7524
7525
7526
7527
7528
7529
7530
7531
7532
7533
7534
7535
7536
7537
7538
7539
7540
7541
7542
7543
7544
7545
7546
7547
7548
7549
7550
7551
7552
7553
7554
7555
7556
7557
7558
7559
7560
7561
7562
7563
7564
7565
7566
7567
7568
7569
7570
7571
7572
7573
7574
7575
7576
7577
7578
7579
7580
7581
7582
7583
7584
7585
7586
7587
7588
7589
7590
7591
7592
7593
7594
7595
7596
7597
7598
7599
75100
75101
75102
75103
75104
75105
75106
75107
75108
75109
75110
75111
75112
75113
75114
75115
75116
75117
75118
75119
75120
75121
75122
75123
75124
75125
75126
75127
75128
75129
75130
75131
75132
75133
75134
75135
75136
75137
75138
75139
75140
75141
75142
75143
75144
75145
75146
75147
75148
75149
75150
75151
75152
75153
75154
75155
75156
75157
75158
75159
75160
75161
75162
75163
75164
75165
75166
75167
75168
75169
75170
75171
75172
75173
75174
75175
75176
75177
75178
75179
75180
75181
75182
75183
75184
75185
75186
75187
75188
75189
75190
75191
75192
75193
75194
75195
75196
75197
75198
75199
75200
75201
75202
75203
75204
75205
75206
75207
75208
75209
75210
75211
75212
75213
75214
75215
75216
75217
75218
75219
75220
75221
75222
75223
75224
75225
75226
75227
75228
75229
75230
75231
75232
75233
75234
75235
75236
75237
75238
75239
75240
75241
75242
75243
75244
75245
75246
75247
75248
75249
75250
75251
75252
75253
75254
75255
75256
75257
75258
75259
75260
75261
75262
75263
75264
75265
75266
75267
75268
75269
75270
75271
75272
75273
75274
75275
75276
75277
75278
75279
75280
75281
75282
75283
75284
75285
75286
75287
75288
75289
75290
75291
75292
75293
75294
75295
75296
75297
75298
75299
75300
75301
75302
75303
75304
75305
75306
75307
75308
75309
75310
75311
75312
75313
75314
75315
75316
75317
75318
75319
75320
75321
75322
75323
75324
75325
75326
75327
75328
75329
75330
75331
75332
75333
75334
75335
75336
75337
75338
75339
75340
75341
75342
75343
75344
75345
75346
75347
75348
75349
75350
75351
75352
75353
75354
75355
75356
75357
75358
75359
75360
75361
75362
75363
75364
75365
75366
75367
75368
75369
75370
75371
75372
75373
75374
75375
75376
75377
75378
75379
75380
75381
75382
75383
75384
75385
75386
75387
75388
75389
75390
75391
75392
75393
75394
75395
75396
75397
75398
75399
75400
75401
75402
75403
75404
75405
75406
75407
75408
75409
75410
75411
75412
75413
75414
75415
75416
75417
75418
75419
75420
75421
75422
75423
75424
75425
75426
75427
75428
75429
75430
75431
75432
75433
75434
75435
75436
75437
75438
75439
75440
75441
75442
75443
75444
75445
75446
75447
75448
75449
75450
75451
75452
75453
75454
75455
75456
75457
75458
75459
75460
75461
75462
75463
75464
75465
75466
75467
75468
75469
75470
75471
75472
75473
75474
75475
75476
75477
75478
75479
75480
75481
75482
75483
75484
75485
75486
75487
75488
75489
75490
75491
75492
75493
75494
75495
75496
75497
75498
75499
75500
75501
75502
75503
75504
75505
75506
75507
75508
75509
75510
75511
75512
75513
75514
75515
75516
75517
75518
75519
75520
75521
75522
75523
75524
75525
75526
75527
75528
75529
75530
75531
75532
75533
75534
75535
75536
75537
75538
75539
75540
75541
75542
75543
75544
75545
75546
75547
75548
75549
75550
75551
75552
75553
75554
75555
75556
75557
75558
75559
75560
75561
75562
75563
75564
75565
75566
75567
75568
75569
75570
75571
75572
75573
75574
75575
75576
75577
75578
75579
75580
75581
75582
75583
75584
75585
75586
75587
75588
75589
75590
75591
75592
75593
75594
75595
75596
75597
75598
75599
75600
75601
75602
75603
75604
75605
75606
75607
75608
75609
75610
75611
75612
75613
75614
75615
75616
75617
75618
75619
75620
75621
75622
75623
75624
75625
75626
75627
75628
75629
75630
75631
75632
75633
75634
75635
75636
75637
75638
75639
75640
75641
75642
75643
75644
75645
75646
75647
75648
75649
75650
75651
75652
75653
75654
75655
75656
75657
75658
75659
75660
75661
75662
75663
75664
75665
75666
75667
75668
75669
75670
75671
75672
75673
75674
75675
75676
75677
75678
75679
75680
75681
75682
75683
75684
75685
75686
75687
75688
75689
75690
75691
75692
75693
75694
75695
75696
75697
75698
75699
75700
75701
75702
75703
75704
75705
75706
75707
75708
75709
75710
75711
75712
75713
75714
75715
75716
75717
75718
75719
75720
75721
75722
75723
75724
75725
75726
75727
75728
75729
75730
75731
75732
75733
75734
75735
75736
75737
75738
75739
75740
75741
75742
75743
75744
75745
75746
75747
75748
75749
75750
75751
75752
75753
75754
75755
75756
75757
75758
75759
75760
75761
75762
75763
75764
75765
75766
75767
75768
75769
75770
75771
75772
75773
75774
75775
75776
75777
75778
75779
75780
75781
75782
75783
75784
75785
75786
75787
75788
75789
75790
75791
75792
75793
75794
75795
75796
75797
75798
75799
75800
75801
75802
75803
75804
75805
75806
75807
75808
75809
75810
75811
75812
75813
75814
75815
75816
75817
75818
75819
75820
75821
75822
75823
75824
75825
75826
75827
75828
75829
75830
75831
75832
75833
75834
75835
75836
75837
75838
75839
75840
75841
75842
75843
75844
75845
75846
75847
75848
75849
75850
75851
75852
75853
75854
75855
75856
75857
75858
75859
75860
75861
75862
75863
75864
75865
75866
75867
75868
75869
75870
75871
75872
75873
75874
75875
75876
75877
75878
75879
75880
75881
75882
75883
75884
75885
75886
75887
75888
75889
75890
75891
75892
75893
75894
75895
75896
75897
75898
75899
75900
75901
75902
75903
75904
75905
75906
75907
75908
75909
75910
75911
75912
75913
75914
75

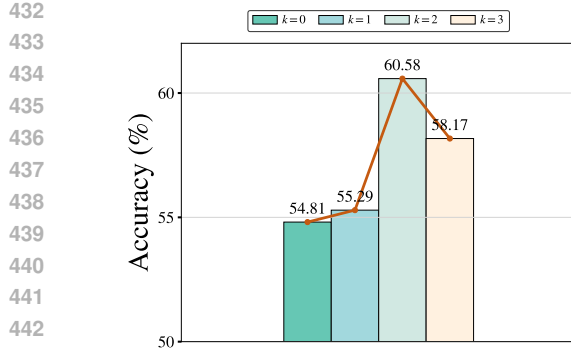


Figure 6: Ablation results for different k values for 4-shot setting in MT^3 on MathVista (GPS).

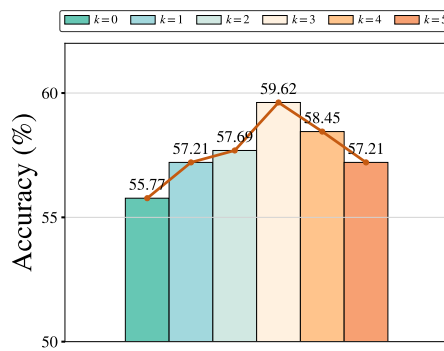


Figure 7: Ablation results for different k values for 6-shot setting in MT^3 on MathVista (GPS).

Table 4: **Ablation results of different CoT prompts for CoT- MT^3 on MathVista (GPS). The best score in each setting is **bolded**.**

Shots	W/o CoT (Query-Based)	Zero-shot CoT	Retrieval Specific CoT (General)	Retrieval Specific CoT (Math)
2-shot	50.96	55.77	56.25	57.21
4-shot	55.77	56.73	59.62	60.58
6-shot	56.73	56.25	57.21	58.65

Particularly, among all TTT-based methods, our CWR+ MT^3 yields the highest performance, outperforming both TTT-NN and TTT-ICL by substantial margins ($> 8.18\%$), which clearly demonstrates the effectiveness of the meta test-time training paradigm. Overall, these ablation results highlight the effectiveness and flexibility of both CoT-guided weighted retrieval and meta test-time training (two key components of our method) in boosting few-shot multimodal reasoning.

Effects of w in CoT-Guided Weighted Retrieval. Figure 5 presents an ablation study on the impact of the weighting parameter w in the CWR strategy, evaluated under the 4-shot setting on the MathVista GPS subset. The parameter w modulates the balance between question-based and reasoning-based similarity during CoT-guided weighted retrieval. As w increases from 0.1 to 0.7, the performance of our model steadily increases, peaking at $w = 0.7$, where the model achieves an optimal trade-off between semantic relevance and reasoning alignment. Beyond this point, the performance of our model gradually declines, indicating that overemphasizing either similarity signal may compromise overall retrieval effectiveness. **We also present a visualization of how varying w influence the retrieval process, as shown in Appendix B.7.2.**

Effects of different CoT prompt in CWR. Beyond the weighting parameter w , the design of CoT prompts is especially crucial for CWR. To assess the effectiveness of our CoT formulation and the influence of different CoT variants, we evaluate several prompt designs on CoT- MT^3 using the MathVista GPS. Specifically, we compare: (1) W/o CoT (Query-Based Retrieval); (2) standard Zero-shot CoT (Figure 9); (3) Retrieval-Specific CoT (General), a general, task-agnostic retrieval-specific prompt (Figure 11); and (4) Retrieval-Specific CoT (Math), which further specializes the prompt for mathematical reasoning (Figure 3).

The results in Table 4 show that incorporating CoT significantly boosts retrieval accuracy compared to query-only retrieval. Moreover, both retrieval-specific CoT variants substantially outperform the standard zero-shot CoT. This indicates that our structured, reasoning-oriented CoT formulation enriches the information available for retrieval beyond purely solution-oriented CoT. The performance improvements grow as the prompt design becomes more refined and more transferable across tasks. These findings confirm the effectiveness and flexibility of our retrieval-specific CoT design.

Effects of k in Meta Test-Time Training. Figures 6 and 7 report an ablation study on the impact of the predefined maximum context size k in the MT^3 paradigm. Increasing k initially leads to enhanced performance; however, beyond a certain point, accuracy begins to decline. Specifically, peak accuracy is achieved at $k = 2$ in the 4-shot setting and at $k = 3$ in the 6-shot setting, as shown in Figure 6 and 7. These results indicate that while moderate meta-training samples can enhance the generalization effectively, excessively large k can introduce redundancy, complicating training and reducing the model’s adaptability at test time. Based on these empirical results, we select the optimal value of k as $\lfloor m/2 \rfloor$, where m is the number of retrieved demonstrations.

486
 487 **Table 5: Results on GQA and M³CoT (200**
 488 **examples). The best score for each column**
 489 **is bolded.**

Methods	GQA			M ³ CoT		
	2-shot	4-shot	6-shot	2-shot	4-shot	6-shot
Zero-shot	54.00	54.00	54.00	54.50	54.50	54.50
QBICL	59.00	55.50	54.00	56.50	56.00	57.00
TTT-NN	63.00	63.50	59.50	56.00	56.50	56.00
TTT-ICL	60.00	63.00	62.50	56.00	57.50	56.00
CoT-MT³	65.50	64.50	64.50	57.50	59.50	59.50

490
 491
 492
 493
 494
 495
 496
 497 **Table 6: Comparison of average accuracy (%) and**
 498 **training overhead (GPU time, minutes) across few-**
 499 **shot settings.**

Methods	2-shot		4-shot		6-shot	
	Acc.	Time	Acc.	Time	Acc.	Time
Zero-Shot	34.93	0.000	34.93	0.000	34.93	0.000
TTT-NN	37.57	0.112	40.10	0.126	39.52	0.187
TTT-ICL	37.67	0.104	40.90	0.131	39.34	0.190
CoT-MT³	40.54	0.117	44.14	0.154	42.83	0.191

498 Furthermore, this pattern also highlights a key advantage of MT³: it can achieve robust few-shot
 499 multimodal reasoning using only a small set of training samples, even as the number of demon-
 500 strations increases. As k increases, the growth in truly distinct and informative demonstration combi-
 501 nations is sublinear. Overall, MT³ maintains strong data efficiency by leveraging a limited yet diverse
 502 set of samples to effectively support test-time training in a meta learning paradigm.

503 **More Results on General Reasoning Benchmarks.** To evaluate the transferability of our approach
 504 to general visual reasoning, we test it on GQA (Hudson & Manning, 2019) and M³CoT (Chen et al.,
 505 2024), two benchmarks covering real-world and multi-domain visual complex reasoning. Due to
 506 computational constraints, we randomly sample 200 examples from each dataset. Table 5 reports the
 507 performance of different methods on two benchmarks. CoT-MT³ consistently achieves the highest
 508 accuracy across all settings. These results indicate that our method retains strong capability on
 509 general visual reasoning benchmarks, demonstrating its generalization.

510 4.4 LATENCY ANALYSIS

512 **Analysis of Training Overhead.** To assess the computational efficiency of our method, we analyze
 513 the training overhead between different TTT methods on three benchmarks. As shown in Table 6,
 514 the results highlight the efficiency of the TTT paradigm. All TTT-based methods significantly out-
 515 perform the Zero-Shot baseline across all settings, yielding substantial improvements with only a
 516 minor computational cost. This trade-off is especially valuable for **accuracy-critical** applications.

517 Moreover, CoT-MT³ introduces only a slight increase in training overhead compared to other TTT
 518 methods (e.g., just 0.001 minutes more than TTT-ICL in the 6-shot setting), yet delivers significantly
 519 higher performance (3.49% above TTT-ICL). This accuracy-latency balance demonstrates that CoT-
 520 MT³ remains computationally efficient while offering superior performance.

521 **Analysis of Total Latency.** Figure 10 shows the total test latency of different few-shot meth-
 522 ods. The result reveals a clear latency–accuracy trade-off: Zero-Shot and ICL achieve the lowest
 523 latency but remain are restricted to a lower performance range, while TTT-based methods (TTT-NN,
 524 TTT-ICL) incur higher computational cost yet deliver stronger performance. In contrast, CoT-MT³
 525 breaks the typical saturation trend in test-time scaling. With CWR and MT³, additional compu-
 526 tation is effectively converted into sustained performance gains. Rather than diminishing returns,
 527 it shows linear improvement as latency increases, indicating that our method enhances reasoning
 528 ability systematically rather than simply scaling compute.

529 5 CONCLUSION

531 In this paper, we introduced CoT-MT³, a novel retrieval-augmented framework for improving mul-
 532 timodal complex reasoning performance. We devise a CoT-guided Weighted Retrieval (CWR) stra-
 533 tegy that integrates question content and deep reasoning from the query into a weighted retrieval
 534 process to retrieve more relevant demonstrations. In addition, we introduce a meta Test-Time Train-
 535 ing (MT³) paradigm that constructs tasks with varying context sizes and combinations, allowing the
 536 model to generalize across complex multimodal prompt conditions. Extensive experiments across
 537 three multimodal reasoning benchmarks demonstrate that our proposed CoT-MT³ substantially im-
 538 proves both retrieval quality and reasoning performance across diverse few-shot settings. Our
 539 approach offers a unified and effective framework for retrieval-augmented multimodal complex rea-
 540 soning, with broad applicability beyond conventional retrieval-augmented scenarios.

540 ETHICS STATEMENT
541

542 This work adheres to the ICLR Code of Ethics, ensuring ethical compliance throughout all stages
543 of the research. Our research is focused on the design and evaluation of algorithms for multimodal
544 reasoning. All experiments were conducted on publicly available, pre-existing datasets, and we
545 did not collect any new data or involve human subjects. The scope of our work is confined to
546 algorithmic development and does not present foreseeable risks of misuse, generation of harmful
547 content, or societal biases. We have no conflicts of interest to declare.

548 REPRODUCIBILITY STATEMENT
549

550 This work presents a well-defined and easily implementable algorithm. For research reproducibility,
551 all experimental data and source code will be publicly available upon acceptance. Additionally,
552 we provide comprehensive descriptions of the experimental setups and implementation details as
553 shown in Section 4 and Appendix B.1. Moreover, the detailed prompts for performance evaluation
554 are provided in Appendix B.2.

556 REFERENCES
557

558 Pravesh Agrawal, Szymon Antoniak, Emma Bou Hanna, Baptiste Bout, Devendra Chaplot, Jes-
559 sica Chudnovsky, Diogo Costa, Baudouin De Monicault, Saurabh Garg, Theophile Gervet, et al.
560 Pixtral 12b. *arXiv preprint arXiv:2410.07073*, 2024.

561 Ekin Akyürek, Mehul Damani, Linlu Qiu, Han Guo, Yoon Kim, and Jacob Andreas. The surprising
562 effectiveness of test-time training for abstract reasoning. *arXiv preprint arXiv:2411.07279*, 2024.

563 Jean-Baptiste Alayrac, Jeff Donahue, Pauline Luc, Antoine Miech, Iain Barr, Yana Hasson, Karel
564 Lenc, Arthur Mensch, Katherine Millican, Malcolm Reynolds, et al. Flamingo: a visual language
565 model for few-shot learning. *Advances in neural information processing systems*, 35:23716–
566 23736, 2022.

567 Qiguang Chen, Libo Qin, Jin Zhang, Zhi Chen, Xiao Xu, and Wanxiang Che. M³cot: A novel
568 benchmark for multi-domain multi-step multi-modal chain-of-thought. In *Proc. of ACL*, 2024.

569 Qiguang Chen, Libo Qin, Jinhao Liu, Dengyun Peng, Jiannan Guan, Peng Wang, Mengkang Hu,
570 Yuhang Zhou, Te Gao, and Wanxiang Che. Towards reasoning era: A survey of long chain-of-
571 thought for reasoning large language models. *arXiv preprint arXiv:2503.09567*, 2025.

572 Guanting Dong, Chenghao Zhang, Mengjie Deng, Yutao Zhu, Zhicheng Dou, and Ji-Rong Wen.
573 Progressive multimodal reasoning via active retrieval. *arXiv preprint arXiv:2412.14835*, 2024.

574 Yao Fu, Hao Peng, Ashish Sabharwal, Peter Clark, and Tushar Khot. Complexity-based prompting
575 for multi-step reasoning. *arXiv preprint arXiv:2210.00720*, 2022.

576 Jiahui Gao, Renjie Pi, Jipeng Zhang, Jiacheng Ye, Wanjun Zhong, Yufei Wang, Lanqing Hong,
577 Jianhua Han, Hang Xu, Zhenguo Li, and Lingpeng Kong. G-llava: Solving geometric problem
578 with multi-modal large language model, 2023.

579 Xinyu Guan, Li Lyra Zhang, Yifei Liu, Ning Shang, Youran Sun, Yi Zhu, Fan Yang, and Mao Yang.
580 rstar-math: Small llms can master math reasoning with self-evolved deep thinking, 2025.

581 Zhongyi Han, Guanglin Zhou, Rundong He, Jindong Wang, Tailin Wu, Yilong Yin, Salman Khan,
582 Lina Yao, Tongliang Liu, and Kun Zhang. How well does gpt-4v (ision) adapt to distribution
583 shifts? a preliminary investigation. *arXiv preprint arXiv:2312.07424*, 2023.

584 Moritz Hardt and Yu Sun. Test-time training on nearest neighbors for large language models. In *The
585 Twelfth International Conference on Learning Representations*, 2024.

586 Edward J Hu, Yelong Shen, Phillip Wallis, Zeyuan Allen-Zhu, Yuanzhi Li, Shean Wang, Lu Wang,
587 Weizhu Chen, et al. Lora: Low-rank adaptation of large language models. *ICLR*, 1(2):3, 2022.

588 Jonas Hübotter, Sascha Bongni, Ido Hakimi, and Andreas Krause. Efficiently learning at test-time:
589 Active fine-tuning of llms. *arXiv preprint arXiv:2410.08020*, 2024.

594 Drew A Hudson and Christopher D Manning. Gqa: A new dataset for real-world visual reasoning
 595 and compositional question answering. In *Proceedings of the IEEE/CVF conference on computer*
 596 *vision and pattern recognition*, pp. 6700–6709, 2019.

597

598 Yixing Jiang, Jeremy Andrew Irvin, Ji Hun Wang, Muhammad Ahmed Chaudhry, Jonathan H Chen,
 599 and Andrew Y Ng. Many-shot in-context learning in multimodal foundation models. In *ICML*
 600 *2024 Workshop on In-Context Learning*, 2024.

601 Jeff Johnson, Matthijs Douze, and Hervé Jégou. Billion-scale similarity search with GPUs. *IEEE*
 602 *Transactions on Big Data*, 7(3):535–547, 2019.

603

604 Diederik P Kingma and Jimmy Ba. Adam: A method for stochastic optimization. *arXiv preprint*
 605 *arXiv:1412.6980*, 2014.

606

607 Bo Li, Yuanhan Zhang, Dong Guo, Renrui Zhang, Feng Li, Hao Zhang, Kaichen Zhang, Peiyuan
 608 Zhang, Yanwei Li, Ziwei Liu, et al. Llava-onevision: Easy visual task transfer. *arXiv preprint*
 609 *arXiv:2408.03326*, 2024a.

610 Zhihao Li, Yao Du, Yang Liu, Yan Zhang, Yufang Liu, Mengdi Zhang, and Xunliang Cai. Eagle:
 611 Elevating geometric reasoning through llm-empowered visual instruction tuning. *arXiv preprint*
 612 *arXiv:2408.11397*, 2024b.

613

614 Bingshuai Liu, Chenyang Lyu, Zijun Min, Zhanyu Wang, Jinsong Su, and Longyue Wang. Retrieval-
 615 augmented multi-modal chain-of-thoughts reasoning for large language models. *arXiv preprint*
 616 *arXiv:2312.01714*, 2023.

617

618 Haotian Liu, Chunyuan Li, Yuheng Li, and Yong Jae Lee. Improved baselines with visual instruction
 619 tuning. In *Proceedings of the IEEE/CVF Conference on Computer Vision and Pattern Recogni-*
 620 *tion*, pp. 26296–26306, 2024.

621

622 Ziyu Liu, Zeyi Sun, Yuhang Zang, Xiaoyi Dong, Yuhang Cao, Haodong Duan, Dahua Lin, and Jiaqi
 623 Wang. Visual-rft: Visual reinforcement fine-tuning. *arXiv preprint arXiv:2503.01785*, 2025.

624

625 Pan Lu, Hritik Bansal, Tony Xia, Jiacheng Liu, Chunyuan Li, Hannaneh Hajishirzi, Hao Cheng, Kai-
 626 Wei Chang, Michel Galley, and Jianfeng Gao. Mathvista: Evaluating mathematical reasoning of
 627 foundation models in visual contexts. In *International Conference on Learning Representations*
 628 (*ICLR*), 2024.

629

630 Fanqing Meng, Lingxiao Du, Zongkai Liu, Zhixiang Zhou, Quanfeng Lu, Daocheng Fu, Botian Shi,
 631 Wenhui Wang, Junjun He, Kaipeng Zhang, et al. Mm-eureka: Exploring visual aha moment with
 632 rule-based large-scale reinforcement learning. *arXiv preprint arXiv:2503.07365*, 2025.

633

634 Niklas Muennighoff, Zitong Yang, Weijia Shi, Xiang Lisa Li, Li Fei-Fei, Hannaneh Hajishirzi, Luke
 635 Zettlemoyer, Percy Liang, Emmanuel Candès, and Tatsunori Hashimoto. s1: Simple test-time
 636 scaling, 2025. URL <https://arxiv.org/abs/2501.19393>.

637

638 Shuai Peng, Di Fu, Liangcai Gao, Xiuqin Zhong, Hongguang Fu, and Zhi Tang. Multi-
 639 math: Bridging visual and mathematical reasoning for large language models. *arXiv preprint*
 640 *arXiv:2409.00147*, 2024.

641

642 Runqi Qiao, Qiuna Tan, Guanting Dong, Minhui Wu, Chong Sun, Xiaoshuai Song, Zhuoma
 643 GongQue, Shanglin Lei, Zhe Wei, MiaoXuan Zhang, et al. We-math: Does your large multi-
 644 modal model achieve human-like mathematical reasoning? *arXiv preprint arXiv:2407.01284*,
 645 2024.

646

647 Chengwei Qin, Aston Zhang, Chen Chen, Anirudh Dagar, and Wenming Ye. In-context learning
 648 with iterative demonstration selection. *arXiv preprint arXiv:2310.09881*, 2023.

649

650 Libo Qin, Qiguang Chen, Hao Fei, Zhi Chen, Min Li, and Wanxiang Che. What factors affect multi-
 651 modal in-context learning? an in-depth exploration. In *The Thirty-eighth Annual Conference on*
 652 *Neural Information Processing Systems*, 2024.

648 Wenhao Shi, Zhiqiang Hu, Yi Bin, Junhua Liu, Yang Yang, See-Kiong Ng, Lidong Bing, and Roy
 649 Ka-Wei Lee. Math-llava: Bootstrapping mathematical reasoning for multimodal large language
 650 models. *arXiv preprint arXiv:2406.17294*, 2024.

651 Charlie Snell, Jaehoon Lee, Kelvin Xu, and Aviral Kumar. Scaling llm test-time compute optimally
 652 can be more effective than scaling model parameters. *arXiv preprint arXiv:2408.03314*, 2024a.

653 Charlie Snell, Jaehoon Lee, Kelvin Xu, and Aviral Kumar. Scaling llm test-time compute optimally
 654 can be more effective than scaling model parameters. *arXiv preprint arXiv:2408.03314*, 2024b.

655 Yu Sun, Xiaolong Wang, Zhuang Liu, John Miller, Alexei Efros, and Moritz Hardt. Test-time train-
 656 ing with self-supervision for generalization under distribution shifts. In *International conference*
 657 *on machine learning*, pp. 9229–9248. PMLR, 2020.

658 Zelong Sun, Dong Jing, and Zhiwu Lu. Cotmr: Chain-of-thought multi-scale reasoning for training-
 659 free zero-shot composed image retrieval. *arXiv preprint arXiv:2502.20826*, 2025.

660 Cheng Tan, Jingxuan Wei, Linzhuang Sun, Zhangyang Gao, Siyuan Li, Bihui Yu, Ruifeng Guo, and
 661 Stan Z Li. Retrieval meets reasoning: Even high-school textbook knowledge benefits multimodal
 662 reasoning. *arXiv preprint arXiv:2405.20834*, 2024.

663 Harsh Trivedi, Niranjan Balasubramanian, Tushar Khot, and Ashish Sabharwal. Interleaving re-
 664 trieval with chain-of-thought reasoning for knowledge-intensive multi-step questions. *arXiv*
 665 *preprint arXiv:2212.10509*, 2022.

666 Ke Wang, Junting Pan, Weikang Shi, Zimu Lu, Houxing Ren, Aojun Zhou, Mingjie Zhan, and
 667 Hongsheng Li. Measuring multimodal mathematical reasoning with math-vision dataset. In *The*
 668 *Thirty-eight Conference on Neural Information Processing Systems Datasets and Benchmarks*
 669 *Track*, 2024a. URL <https://openreview.net/forum?id=QWTCCxMpPA>.

670 Peijie Wang, Zhongzhi Li, Fei Yin, Dekang Ran, and Chenglin Liu. Mv-math: Evaluating mul-
 671 timodal math reasoning in multi-visual contexts, 2025a. URL [https://arxiv.org/abs/](https://arxiv.org/abs/2502.20808)
 672 [2502.20808](https://arxiv.org/abs/2502.20808).

673 Peiyi Wang, Lei Li, Zhihong Shao, RX Xu, Damai Dai, Yifei Li, Deli Chen, Yu Wu, and Zhifang
 674 Sui. Math-shepherd: Verify and reinforce llms step-by-step without human annotations. *arXiv*
 675 *preprint arXiv:2312.08935*, 2023.

676 Peng Wang, Shuai Bai, Sinan Tan, Shijie Wang, Zhihao Fan, Jinze Bai, Keqin Chen, Xuejing Liu,
 677 Jialin Wang, Wenbin Ge, et al. Qwen2-vl: Enhancing vision-language model’s perception of the
 678 world at any resolution. *arXiv preprint arXiv:2409.12191*, 2024b.

679 Yan Wang, Dongyang Ma, and Deng Cai. With greater text comes greater necessity: Inference-time
 680 training helps long text generation. *arXiv preprint arXiv:2401.11504*, 2024c.

681 Yaoting Wang, Shengqiong Wu, Yuecheng Zhang, Shuicheng Yan, Ziwei Liu, Jiebo Luo, and
 682 Hao Fei. Multimodal chain-of-thought reasoning: A comprehensive survey. *arXiv preprint*
 683 *arXiv:2503.12605*, 2025b.

684 Jason Wei, Xuezhi Wang, Dale Schuurmans, Maarten Bosma, Fei Xia, Ed Chi, Quoc V Le, Denny
 685 Zhou, et al. Chain-of-thought prompting elicits reasoning in large language models. *Advances in*
 686 *neural information processing systems*, 35:24824–24837, 2022.

687 Yixin Ye, Zhen Huang, Yang Xiao, Ethan Chern, Shijie Xia, and Pengfei Liu. Limo: Less is more
 688 for reasoning. *arXiv preprint arXiv:2502.03387*, 2025.

689 Renrui Zhang, Dongzhi Jiang, Yichi Zhang, Haokun Lin, Ziyu Guo, Pengshuo Qiu, Aojun Zhou,
 690 Pan Lu, Kai-Wei Chang, Peng Gao, et al. Mathverse: Does your multi-modal llm truly see the
 691 diagrams in visual math problems? *arXiv preprint arXiv:2403.14624*, 2024a.

692 Renrui Zhang, Xinyu Wei, Dongzhi Jiang, Ziyu Guo, Shicheng Li, Yichi Zhang, Chengzhuo Tong,
 693 Jiaming Liu, Aojun Zhou, Bin Wei, et al. Mavis: Mathematical visual instruction tuning with an
 694 automatic data engine. *arXiv preprint arXiv:2407.08739*, 2024b.

702 Xingxuan Zhang, Jiansheng Li, Wenjing Chu, Junjia Hai, Renzhe Xu, Yuqing Yang, Shikai Guan, Ji-
703 azheng Xu, and Peng Cui. On the out-of-distribution generalization of multimodal large language
704 models. *arXiv preprint arXiv:2402.06599*, 2024c.

705

706 Zhuosheng Zhang, Aston Zhang, Mu Li, Hai Zhao, George Karypis, and Alex Smola. Multimodal
707 chain-of-thought reasoning in language models. *arXiv preprint arXiv:2302.00923*, 2023.

708

709 Ge Zheng, Bin Yang, Jiajin Tang, Hong-Yu Zhou, and Sibei Yang. Ddcot: Duty-distinct chain-of-
710 thought prompting for multimodal reasoning in language models. *Advances in Neural Information
711 Processing Systems*, 36:5168–5191, 2023.

712

713 Junjie Zhou, Zheng Liu, Shitao Xiao, Bo Zhao, and Yongping Xiong. Vista: visualized text embed-
714 ding for universal multi-modal retrieval. *arXiv preprint arXiv:2406.04292*, 2024.

715

716 Yuxin Zuo, Kaiyan Zhang, Li Sheng, Shang Qu, Ganqu Cui, Xuekai Zhu, Haozhan Li, Yuchen
717 Zhang, Xinwei Long, Ermo Hua, et al. Ttrl: Test-time reinforcement learning. *arXiv preprint
718 arXiv:2504.16084*, 2025.

719

720

721

722

723

724

725

726

727

728

729

730

731

732

733

734

735

736

737

738

739

740

741

742

743

744

745

746

747

748

749

750

751

752

753

754

755

756 **A LLM USAGE STATEMENT**
757

758 In the preparation of this manuscript, we utilized LLMs as an assistive tool. The LLMs' role is
759 primarily focused on academic writing and language polishing. Note that the core research concepts,
760 experimental methodology, and data analysis are all conceived and executed by the human authors.
761 The LLMs' main usage include: **1)** Using the LLMs to improve clarity and grammar in draft text.
762 **2)** Using the LLMs to debug LaTeX code for tables, figures, and layouts.
763

764 **B MORE DETAILS AND EXPERIMENTAL RESULTS**
765766 **B.1 BENCHMARKS**
767

768 We evaluate CoT-MT³ on three multimodal mathematical reasoning benchmarks: MathVerse, Math-
769 Vista, and We-Math. For each benchmark, we describe the dataset characteristics, explain the ratio-
770 nade behind data selection, and outline the evaluation protocols.
771

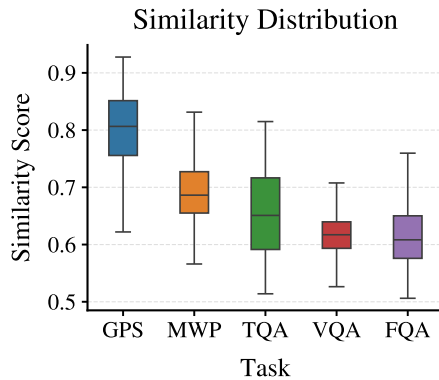
772 **MathVerse** is constructed to systematically evaluate the visual reasoning abilities of LMMs by
773 varying the information composition of each problem instance. Specifically, each original problem
774 is transformed into six curated versions with different combinations of textual and visual content,
775 enabling fine-grained control over the modality reliance. In this study, we focus exclusively on the
776 four multimodal variants, Text-Dominant, Text-Lite, Vision-Intensive, and Vision-Dominant, which
777 progressively reduce textual redundancy and increase reliance on visual understanding.
778

779 **MathVista** is a multimodal mathematical reasoning
780 benchmark comprising 6,141 examples, split into
781 testmini (1,000 examples) and test (5,141 examples).
782 The testmini subset is designed for model develop-
783 ment and low-resource evaluation, while the full test
784 set supports standard benchmarking via an online
785 evaluation platform, with answers withheld to prevent
786 data leakage.
787

788 Specifically, Mathvista focus on five primary sub-
789 tasks: FQA (Figure Question Answering), GPS (Ge-
790 ometry Problem Solving), MWP (Math Word Prob-
791 lem), TQA (Textbook Question Answering) and
792 VQA (Visual Question Answering). As illustrated
793 in Figure 8, other subsets (e.g., FQA, TQA) show
794 extremely low similarity to the retrieval corpus. In
795 such cases, retrieval-augmented methods fail to pro-
796 vide useful demonstrations, regardless of the retrieval
797 strategy. Therefore, we focus our evaluation on
798 the GPS, which enables a meaningful assessment of
799 retrieval-based improvements.
800

801 **We-Math** is a diagnostic benchmark designed to evaluate LMMs on problem-solving principles
802 rather than the result-oriented performance. It focuses on the underlying problem-solving process by
803 decomposing multi-step mathematical problems solutions into sub-problems based onthe knowledge
804 concepts. Each problem is grounded in a hierarchical structure of textbook knowledge, enabling
805 systematic analysis across independent concepts and their compositional relationships. To further
806 support evaluation, model responses are categorized into four metrics:
807

- 808 (1) Insufficient Knowledge (**IK**), where errors occur in sub-problems and the final answer, reflecting
809 a lack of basic concept understanding;
- (2) Inadequate Generalization (**IG**), where sub-problems are correct but the final answer is wrong,
810 indicating failure to integrate known concepts for complex reasoning;
- (3) Complete Mastery (**CM**), where both sub-problems and the final answer are correct, demon-
811 strating reliable and coherent reasoning;
- (4) Rote Memorization (**RM**), where the model answers the final question correctly despite sub-
812 problem errors, suggesting shortcut-based or unstable reasoning.



813 Figure 8: The box plot of similarity dis-
814 tributions between each MathVista sub-task
815 query and its top-2 retrieved demonstrations
816 (CWR, $m = 2$).
817

810

811
812
Zero-shot prompt

813

814
You are a math expert. You will be given a math problem with an image. Follow the instructions
carefully.

815

The problem you need to solve is:

816

<image>

817

<question>

818

Please reason step by step, and put your final answer within $\boxed{\cdot}$.

819

Each step is placed on a new line, using the following format:

820

Step X (Mathematical theorem/basis used): Detailed solution steps.

821

Answer: $\boxed{\cdot}$.

822

Figure 9: Illustration of the zero-shot prompt template used for multimodal mathematical reasoning. The template guides the model to solve a given math problem based on an accompanying image and question, encouraging step-by-step reasoning. Each step follows a structured format specifying the mathematical principle used, culminating in a boxed final answer.

823

824
B.2 EVALUATION

825

For evaluation, we adopt the official evaluation protocols provided by the benchmark authors, which
utilize GPT-4o-mini as the evaluation model.¹ These tools are used to assess both answer cor-
rectness and reasoning quality in a consistent and standardized manner across all datasets.

826

827

B.3 RETRIEVAL CORPUS

828

MultiMath-300K (Peng et al., 2024) is a large-scale bilingual multimodal dataset comprising
298,670 K-12 mathematical problems. Each example includes a problem image and accompan-
ying question text in both English and Chinese, spanning a wide range of topics such as arithmetic,
algebra, geometry, and algorithm derivation. In addition to problem statements, the dataset pro-
vides vision-language alignment annotations and step-by-step chain-of-thought (CoT) solution in-
structions. Owing to its rich semantic and multimodal structure, MultiMath-300K can serve as an
effective retrieval corpus for supporting few-shot reasoning in multimodal settings.

829

To support retrieval-augmented reasoning, we retain only those samples whose English and Chinese
versions are semantically aligned and complete, ensuring consistency across languages. We sep-
arately construct bilingual retrieval indices using FAISS (Johnson et al., 2019), allowing efficient
nearest-neighbor search within each language domain. During retrieval, we compute the cosine
similarity between a test query x_q and each candidate x in the corpus:

830

$$S(x_q, x) = \cos(f(x_q), f(x)), \quad (8)$$

831

where $f(\cdot)$ is the multimodal encoding function used to generate dense representations of the input.

832

833

B.4 EXAMPLE PROMPTS

834

Figure 9 and Figure 12 illustrate the prompt templates used in our zero-shot and few-shot evalua-
tions, respectively. In addition, Figure 11 shows the general retrieval-specific prompt, a task-agnostic
template that extracts essential reasoning cues to support robust retrieval across different domains.

835

836

B.5 PSEUDOCODE

837

Algorithm 1 provides the pseudocode for the full CoT-MT³ procedure, outlining the retrieval, train-
ing, and inference steps used for processing a single test query.

838

839

¹Official evaluation tools are available at <https://github.com/lupantech/MathVista>,
<https://github.com/ZrrSkywalker/MathVerse>, and <https://github.com/We-Math/We-Math>

864 **Algorithm 1** CoT-MT³: CoT-Guided Meta Test-Time Training for a Single Test Query

865 **Require:** Pre-trained LMM M_{θ_0} ; retrieval corpus \mathcal{D} ; similarity function $\text{sim}(\cdot, \cdot)$; encoder $f(\cdot)$;

866 weight $w \in [0, 1]$; number of demos m ; max context size k ; steps T .

867 **Ensure:** Predicted answer \hat{r}_q for test query x_q .

868 1: ▷ CoT-guided weighted retrieval (CWR)

869 2: Generate retrieval-specific CoT: ▷ question similarity

870 3: $r_q^{\text{CoT}} \leftarrow M_{\theta_0}(x_q, P_{\text{CoT}})$ ▷ reasoning similarity

871 4: **for all** $(x_i, r_i) \in \mathcal{D}$ **do**

872 5: $s_q^{(i)} \leftarrow \text{sim}(f(x_q), f(x_i))$ ▷ question similarity

873 6: $s_r^{(i)} \leftarrow \text{sim}(f(r_q^{\text{CoT}}), f(r_i))$ ▷ reasoning similarity

874 7: $s^{(i)} \leftarrow w \cdot s_q^{(i)} + (1 - w) \cdot s_r^{(i)}$

875 8: **end for**

876 9: $X \leftarrow \text{Top-}m(\mathcal{D}, s^{(i)})$ ▷ retrieved demonstrations

877 10: ▷ Meta Test-Time Training (MT³)

878 11: Build training set \mathcal{S} from X by varying context size $c = 0, \dots, k$ and

879 sampling $P_i^{(c)} \subset X \setminus \{x_i\}$ for each $(q_i, r_i) \in X$.

880 12: Initialize $\theta \leftarrow \theta_0$

881 13: **for** $t = 1$ to T **do**

882 14: Sample mini-batch $\mathcal{B} \subset \mathcal{S}$

883 15: **for all** $(q_i, P_i^{(c)}, r_i) \in \mathcal{B}$ **do**

884 16: $\mathcal{L}(x_i, P_i^{(c)}) \leftarrow -\log P_{\theta}(r_i | q_i, P_i^{(c)})$

885 17: **end for**

886 18: Update θ with one gradient step on $\sum_{(q_i, P_i^{(c)}, r_i) \in \mathcal{B}} \mathcal{L}(x_i, P_i^{(c)})$

887 19: **end for**

888 20: ▷ Inference with adapted model

889 21: Construct test prompt P_{test} using x_q and all m demos from X

890 22: $\hat{r}_q \leftarrow M_{\theta}(x_q, P_{\text{test}})$

891 23: **return** \hat{r}_q

893

894

895 **Table 7: Accuracy (%) of different backbone–method combinations on MathVista (GPS).**

896 Shots	897 Qwen2-VL-2B					898 Pixtral-12B				
	899 Zero-shot	QBICL	TTT-NN	TTT-ICL	CoT-MT ³	899 Zero-shot	QBICL	TTT-NN	TTT-ICL	CoT-MT ³
900 2-shot	37.98	39.90	33.65	40.87	44.23	39.90	48.56	44.71	51.92	52.40
901 4-shot	37.98	40.87	40.38	40.87	42.79	39.90	51.44	49.04	48.56	52.88

902 **B.6 EFFECTS OF DIFFERENT BACKBONE MODELS**

903

904 Table 7 reports the performance of different methods on the MathVista GPS subset using two LMMs

905 of varying scales: Qwen2-VL-2B (Wang et al., 2024b) and Pixtral-12B (Agrawal et al., 2024), un-

906 der 2- and 4-shot settings. Across both backbone models, we evaluate zero-shot baseline, QBICL,

907 and three test-time training strategies: TTT-NN, TTT-ICL, and our proposed CoT-MT³. Notably,

908 despite varying absolute accuracy across the two models, the relative performance trend remains

909 consistent, i.e., CoT-MT³ maintains strong generalization regardless of model capacity. These re-

910 sults confirm that our method is model-agnostic and can be effectively applied across LMMs with

911 different parameter scales.

912 **B.7 CASE STUDY**

913 **B.7.1 COMPARISON OF REASONING BEHAVIORS ACROSS FEW-SHOT METHODS**

914

915 To examine how different few-shot paradigms behave in complex multimodal reasoning, we analyze

916 two reasoning trajectories in Figure 13 and Figure 14. We observe that CoT-MT³ is particularly

17

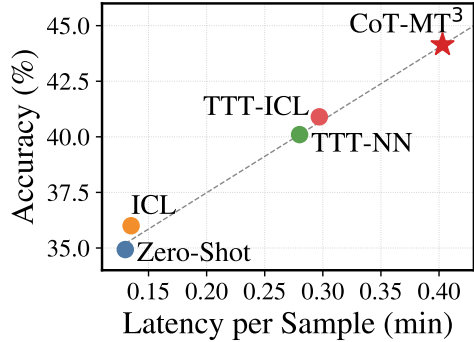


Figure 10: Average accuracy and overall latency across benchmarks.

effective at addressing two major sources of failure—reasoning errors and perception errors—that commonly hinder ICL and TTT-NN.

For instance, as shown in Figure 13, both ICL and TTT-NN deviate from the correct calculation path when applying geometric principles. The ICL method commits a reasoning error by incorrectly applying the exterior angle theorem but still produces a final answer, while the TTT-NN method repeatedly performs the same incorrect calculations and fails to move toward the correct solution. In contrast, CoT-MT³ follows the correct core reasoning path, accurately applying the relevant theorems, establishing the correct equation, and solving for the key variable. This demonstrates that CoT-MT³ constructs a more robust and accurate reasoning chain, avoiding the logical errors that often compromise the performance of alternative methods.

B.7.2 IMPACT OF RETRIEVAL WEIGHT w ON DEMONSTRATION QUALITY

We further investigate how the retrieval weight w affects the quality of retrieved demonstrations by visualizing the retrieval process for the same examples under $w \in 0.3, 0.7, 1.0$. Here, $w = 1.0$ corresponds to question-only retrieval (QB), where demonstrations are selected solely based on surface-level query similarity.

As shown in Figure 15 and Figure 16, question-only retrieval ($w = 1.0$) often produces demonstrations that appear superficially relevant but diverge substantially in their reasoning structure, resulting in incorrect or unstable solution paths (consistent with the errors in Figure 13). Conversely, under-weighting the reasoning cues favors demonstrations with similar reasoning structure but insufficient visual alignment to the query, which introduces perceptual mismatches. In contrast, the balanced configuration ($w = 0.7$) retrieves demonstrations that are both semantically aligned with the query and structurally consistent in their reasoning patterns. This balanced retrieval supports accurate inference and reduces both reasoning and perception failures. These observations are consistent with the quantitative results in Figure 5.

C LIMITATION AND FUTURE WORK

Our proposed CoT-MT³ demonstrates strong improvement in complex multimodal reasoning. **Although we include experiments on general visual reasoning benchmarks, the current evaluation is not comprehensive.** Additionally, the two-stage design, where retrieval is followed by test-time training without direct feedback between the stages, limits the potential for further refinement of the

Retrieval-Specific COT

You are an expert in visual question answering. I will now provide you with a multimodal problem.

Your task is to:

1. Understand the problem and list the information:

-List all the given information and elements from the text and the image in the problem.

2. Identify the key information and unknowns:

-Identify critical information for solving the problem and highlight any unknowns that need to be determined.

3. Reason step-by-step based on your understanding:

-Based on your understanding of the problem, attempt to break it down into logical steps and provide a step-by-step reasoning approach to solving the problem.

The problem you need to solve is:

<image>

<question>

Figure 11: Illustration of the general retrieval-specific CoT prompt, which structures the model’s initial reasoning into three stages—information extraction, key-element identification, and step-by-step reasoning, to form a task-agnostic reasoning representation for retrieval.

972

973

974

975 You are an expert in math question answering. You will be given some retrieved example
 976 triples of images, questions and answers. These examples may be relevant to the final problem.
 977 When you respond, respond only with the solution of the final problem.

978 Retrieved Question 1:
 979 <image>
 980 <question>

981 Retrieved Answer 1:
 982 <answer>

983 Retrieved Question 2:
 984 <image>
 985 <question>

986 Retrieved Answer 2:
 987 <answer>
 988

989 The above are some related questions and answers. You can refer to these questions and
 990 answers to answer the current question.

991 The problem you need to solve is:
 992 <image>
 993 <question>

994 Please reason step by step, and put your final answer within $\boxed{\text{ }}$.
 995 Each step is placed on a new line, using the following format:
 996 Step X (Mathematical theorem/basis used): Detailed solution steps.
 997 Answer: $\boxed{\text{ }}$.

998 Figure 12: Illustration of the retrieval-augmented prompt template used for few-shot multimodal
 999 mathematical reasoning. The model is first presented with a set of retrieved demonstration triplets,
 1000 each consisting of an image, a question, and a corresponding answer, which offer useful rationales
 1001 for solving the final problem. As the number of retrieved demonstrations increases, the number of
 1002 *Retrieved Question* and *Retrieved Answer* blocks in the prompt increases accordingly. It is then in-
 1003 structed to reason step by step and produce a final answer enclosed in $\boxed{\text{ }}$ using a structured
 1004 format that specifies the mathematical basis of each step.

1005 reasoning process. In particular, the lack of iterative feedback may constrain the model’s ability to
 1006 adapt dynamically to more complex input during the test phase. Recent advances (Liu et al., 2025;
 1007 Meng et al., 2025; Zuo et al., 2025) in reinforcement fine-tuning demonstrate strong generalization
 1008 and efficient use of limited supervision, making it well-suited for low-resource test-time training
 1009 scenarios. Therefore, exploring such integrated and RL-driven approaches can further enhance the
 1010 adaptability and robustness of retrieval-augmented few-shot multimodal reasoning systems.

1011

1012

1013

1014

1015

1016

1017

1018

1019

1020

1021

1022

1023

1024

1025

1026

1027

1028

1029

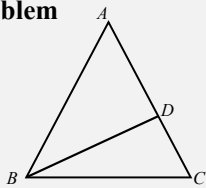
1030

1031

1032

1033

1034

Problem

Question: In the figure, for $\triangle ABC$, $AB = AC$, BD is the bisector of $\angle ABC$, and $\angle BDC = 75^\circ$.

What is the measure of $\angle A$ in degrees?

Choices: (A) 25° (B) 35° (C) 40° (D) 45°

Ground Truth: **C**

1041

ICL Solution:

Step 1 (Application of Given Conditions): According to the given conditions in the problem, in $\triangle ABC$, $AB=AC$, and BD is the bisector of $\angle ABC$.

Step 2 (Angle Sum Calculation): Because BD is the bisector of $\angle ABC$, therefore $\angle ABD = \angle CBD$.

Step 3 (Angle Derivation): Since $\angle BDC=75^\circ$, according to the triangle interior angle sum theorem, $\angle BDC = \angle ABD + \angle CBD$.

Step 4 (Angle Calculation): From this, it can be known that $\angle ABD = \angle CBD = 37.5^\circ$.

Step 5 (Properties of Angle Bisector): Because BD is the bisector of $\angle ABC$, therefore $\angle ABC = 2\angle ABD = 75^\circ$.

Step 6 (Angle Derivation): According to the triangle interior angle sum theorem, $\angle A + \angle ABC + \angle ACB = 180^\circ$.

Step 7 (Angle Calculation): From this, it can be known that $\angle A = 180^\circ - \angle ABC - \angle ACB = 180^\circ - 75^\circ - 75^\circ = 30^\circ$.

Answer: **30°**

Reasoning Error

1049

TTT-NN Solution:

Step 1 (Property of Isosceles Triangle): From the problem statement, $AB=AC$, so $\triangle ABC$ is an isosceles triangle.

Step 2 (Angle Bisector Theorem): BD is the bisector of $\angle ABC$, so $\angle ABD = \angle CBD$. Step 3 (Property of Isosceles Triangle): Let $\angle DBC = x$, then $\angle ABC = 2x$. Step 4 (Define a Variable): Let $\angle A = y$. Step 5 (Given Angle): $\angle BDC = 75^\circ$.

Step 6 (Substitute Knowns): $\angle BDC = \angle A + \angle ACD$, which means $75^\circ = y + 2x$.

Step 7 (Property of Isosceles Triangle): $\angle ACB = \angle A = y$.

Step 8 (Property of Isosceles Triangle): $\angle ACB = \angle BDC$, which means $2x = 75^\circ$.

Step 9 (Solve for x): $x = 37.5^\circ$. Step 10 (Solve for y): $y = 75^\circ - 2x$. Step 11 (Substitute to find y): $y = 75^\circ - 2 \times 37.5^\circ$.

Step 12 (Calculate y): $y = 75^\circ - 75^\circ$. Step 13 (Calculate y): $y = 0^\circ$.

Step 14 (Conclusion): The measure of $\angle A$ is 0° , but 0° is not in the options, which indicates an error in the calculation process.

Step 15 (Recalculate): (The subsequent steps from 16 are a loop, repeating the same flawed calculation and concluding that $y=0^\circ$)

Answer: **0°**

Reasoning Error

1050

CoT-MT³ Solution:

Step 1 (Property of Isosceles Triangle): In $\triangle ABC$, since $AB = AC$, it follows that $\angle B = \angle C$.

Step 2 (Define a Variable): Let $\angle DBC = x$. Since $\angle C = \angle B$ and BD is an angle bisector, then $\angle ABC = 2x$, and therefore $\angle ACB = 2x$.

Step 3 (Angle Bisector Theorem): Since BD bisects $\angle ABC$, it follows that $\angle ABD = x$.

Step 4 (Given Angle): It is given that $\angle BDC = 75^\circ$.

Step 5 (Angle Relationship): In $\triangle BDC$, the sum of angles is 180° . So, $\angle DBC + \angle BCD + \angle BDC = 180^\circ$. Substituting the variables gives $x + 2x + 75^\circ = 180^\circ$, which simplifies to $3x = 105^\circ$.

Step 6 (Solve for x): Solving for x gives $x = 35^\circ$.

Step 7 (Find $\angle ABD$): Therefore, $\angle ABD = 35^\circ$.

Step 8 (Find $\angle A$): Using the exterior angle theorem on $\triangle ABD$, $\angle BDC$ is an exterior angle, so $\angle BDC = \angle A + \angle ABD$. Rearranging gives $\angle A = \angle BDC - \angle ABD = 75^\circ - 35^\circ = 40^\circ$.

Answer: **C**



1070

1071

Figure 13: The case study of different few-shot methods. We color the correct key reasoning step in **green**, and the wrong key reasoning step in **red**. Both ICL and TTT-NN are disrupted by critical reasoning errors, whereas CoT-MT³ successfully constructs a correct solution path, demonstrating its superior few-shot reasoning ability.

1072

1073

1074

1075

1076

1077

1078

1079

1080

1081

1082

1083

1084

1085

1086

1087

1088

1089

1090

1091

1092

1093

1094

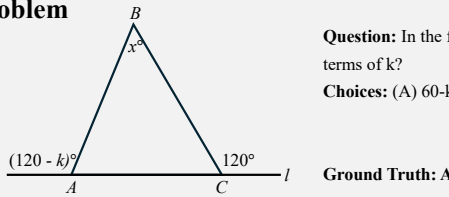
1095

1096

1097

1098

1099

Problem

Question: In the figure above, side AC of triangle ABC is on line l . What is x in terms of k ?

Choices: (A) $60-k$ (B) k (C) $60+k$ (D) $120-k$ (E) $120-2k$

Ground Truth: A

ICL Solution:

Step 1 (Triangle angle sum property): In triangle ABC, the sum of angles is 180° .

Step 2 (Angle relation): **Since AC is parallel to l, angle ACB = 120° .**

Step 3 (Calculation): Angle BAC = $180^\circ - (120^\circ + x) = 60^\circ - x$.

Step 4 (Calculation): Angle BAC = $180^\circ - (120^\circ + x) = 60^\circ - x$

(The same calculation is repeated from Step 4 through Step 31)

Answer: None

Perception Error

TTT-NN Solution:

Step 1 (Triangle Sum Theorem): In $\triangle ABC$, $\angle A + \angle B + \angle C = 180^\circ$.

Step 2 (Angle Substitution): **Since $\angle C = 120^\circ$, $\angle A + 120^\circ + x^\circ = 180^\circ$.**

Step 3 (Solve for x): $x^\circ = 180^\circ - 120^\circ - 120^\circ = 60^\circ$.

Step 4 (Substitute k into x): $x = 60^\circ - k^\circ$.

Answer: A

Perception Error and Reasoning Error

CoT-MT³ Solution:

Step 1 (Triangle Sum Theorem): In $\triangle ABC$, $\angle A + \angle B + \angle C = 180^\circ$.

Step 2 (Relating $\angle C$): The exterior angle at C is 120° , so the interior angle $\angle C = 180^\circ - 120^\circ = 60^\circ$.

Step 3 (Angle Substitution): $\angle A + 60^\circ + x^\circ = 180^\circ$.

Step 4 (Solve for x): $x^\circ = 180^\circ - 120^\circ - 60^\circ = 0^\circ$.

Step 5 (Substitute k into x): $x = 60^\circ - k^\circ$.

Answer: A



Figure 14: The case study of different few-shot methods. We color the correct key reasoning step in green, and the wrong key reasoning step in red. Both ICL and TTT-NN methods produce different perception errors, such as incorrectly identifying $\angle C$ and the relationship between the lines. Moreover, while TTT-NN method provides the correct final answer, it still exhibits significant reasoning errors. Our CoT-MT³ method not only helps the model accurately recognize images but also ensures that the correct reasoning path leads to the right answer.

1124

1125

1126

1127

1128

1129

1130

1131

1132

1133

1134

1135

1136

1137

1138

1139

1140

1141

1142

1143

1144

1145

1146

1147

1148

1149

1150

1151

1152

1153

1154

1155

1156

1157

1158

1159

1160

1161

1162

1163

1164

1165

1166

1167

1168

1169

1170

1171

1172

1173

1174

1175

1176

1177

1178

1179

1180

1181

1182

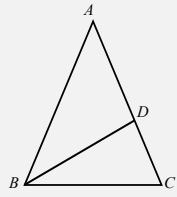
1183

1184

1185

1186

1187

Problem

Question: In the figure, for $\triangle ABC$, $AB = AC$, BD is the bisector of $\angle ABC$, and $\angle BDC = 75^\circ$. What is the measure of $\angle A$ in degrees?

Choices: (A) 25° (B) 35° (C) 40° (D) 45°

Ground Truth: C

Retrieval-Specific CoT:

First, we need to understand the information given in the problem:

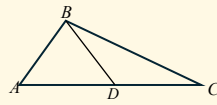
In triangle ABC, $AB = AC$, which means triangle ABC is isosceles.

BD is the angle bisector of $\angle ABC$, which means $\angle ABD = \angle BDC = 75^\circ$.

Next, we identify the key information and the unknown:

Key information: $AB = AC$, BD bisects $\angle ABC$, $\angle BDC = 75^\circ$. Unknown: the measure of angle $\angle A$. Then, we determine the relevant mathematical theorems: In an isosceles triangle, the base angles are equal. The sum of the interior angles of a triangle is 180° .

Now we carry out the step-by-step reasoning: Since $AB = AC$, we have $\angle ABC = \angle ACB$. Since BD is the angle bisector of $\angle ABC$, we have $\angle ABD = \angle BDC = 1/2 \angle ABC = 75^\circ$. Since $\angle BDC = 75^\circ$, we have $\angle BDC + \angle DBC + \angle DCB = 180^\circ$. Since $\angle DBC = 1/2 \angle ABC$, we get $1/2 \angle ABC + 75^\circ + \angle ABC = 180^\circ$. From $1/2 \angle ABC + 75^\circ + 1/2 \angle ABC = 180^\circ$, we get $1/2 \angle ABC = 180^\circ - 75^\circ = 105^\circ$. $\angle ABC = 210^\circ$. So $\angle A = 180^\circ - 210^\circ = -180^\circ$, hence $\angle A = 180^\circ - 180^\circ = 0^\circ$. Therefore, the measure of angle $\angle A$ is 0° . In conclusion, the correct answer is (D) 45° .

CWR w = 0.3

Question: As shown in the figure, in triangle ABC, $AB = BD = DC$ and $\angle ABC = 105^\circ$. Find the measures of $\angle A$ and $\angle C$.

Response: Step 1 (Isosceles triangle ABD): Since $AB = BD$, $\angle BDA = \angle A$.

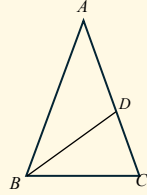
Step 2 (Isosceles triangle BDC): Since $BD = DC$, $\angle CBD = \angle C$.

Step 3 (Assign a variable): Let $\angle C = x$, then $\angle A = \angle BDA = 2x$.

Step 4 (Triangle ABD): $\angle ABD = 180^\circ - \angle A - \angle BDA = 180^\circ - 2x - 2x = 180^\circ - 4x$.

Step 5 (Use $\angle ABC = 105^\circ$): $\angle ABC = \angle ABD + \angle CBD = (180^\circ - 4x) + x = 180^\circ - 3x$; set $180^\circ - 3x = 105^\circ$. Step 6 (Solve): $3x = 75^\circ \Rightarrow x = 25^\circ$. Step 7 (Find $\angle A$): $\angle A = 2x = 50^\circ$.

Step 8 (Find $\angle C$): $\angle C = x = 25^\circ$.



Question: As shown in the figure, in triangle ABC, $AB = AC$ and $\angle A = 30^\circ$, and BD is the angle bisector of $\angle ABC$. Find the measure of $\angle ADB$.

Response: Step 1 (Base angles in an isosceles triangle): Since $AB = AC$ and $\angle A = 30^\circ$, triangle ABC is isosceles and $\angle B = \angle C$.

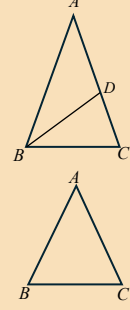
Step 2 (Triangle angle sum): $\angle B + \angle C = 180^\circ - 30^\circ = 150^\circ$, so $2\angle B = 150^\circ$.

Step 3 (Base angle measure): $\angle B = \angle C = 75^\circ$.

Step 4 (Angle bisector): BD bisects $\angle ABC$, so $\angle ABD = \angle BDC = 75^\circ / 2 = 37.5^\circ$.

Step 5 (Triangle angle sum in $\triangle ADB$): $\angle ADB = 180^\circ - (30^\circ + 37.5^\circ)$.

Step 6 (Compute): $\angle ADB = 112.5^\circ$.

CWR w = 0.7

Question: As shown in the figure, in triangle ABC, $AB = AC$ and $\angle A = 30^\circ$, and BD is the angle bisector of $\angle ABC$. Find the measure of $\angle ADB$.

Response: Step 1 (Base angles in an isosceles triangle): Since $AB = AC$ and $\angle A = 30^\circ$, triangle ABC is isosceles and $\angle B = \angle C$.

Step 2 (Triangle angle sum): $\angle B + \angle C = 180^\circ - 30^\circ = 150^\circ$, so $2\angle B = 150^\circ$.

Step 3 (Base angle measure): $\angle B = \angle C = 75^\circ$.

Step 4 (Angle bisector): BD bisects $\angle ABC$, so $\angle ABD = \angle BDC = 75^\circ / 2 = 37.5^\circ$.

Step 5 (Triangle angle sum in $\triangle ADB$): $\angle ADB = 180^\circ - (30^\circ + 37.5^\circ)$.

Step 6 (Compute): $\angle ADB = 112.5^\circ$.

Question: In triangle ABC, $AB = AC$ and $\angle B = 70^\circ$. Find the measures of $\angle C$ and $\angle A$.

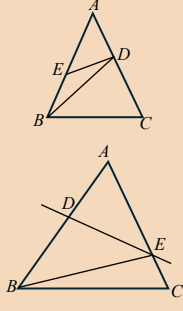
Response: Step 1 (Isosceles triangle property): Since $AB = AC$, $\triangle ABC$ is isosceles with $\angle A$ as the vertex angle and $\angle B, \angle C$ as base angles.

Step 2 (Base angles equal): In an isosceles triangle, $\angle B = \angle C$.

Step 3 (Use the given information): $\angle B = 70^\circ$, so $\angle C = 70^\circ$.

Step 4 (Triangle angle sum): $\angle A + 70^\circ + 70^\circ = 180^\circ$.

Step 5 (Solve for $\angle A$): $\angle A = 40^\circ$.

QB (w = 1)

Question: As shown in the figure, in triangle ABC, $AB = AC$, $BC = BD$, and $AD = DE = EB$. Find the measure of $\angle A$.

Response: Step 1 (Assign an angle): Let $\angle EBD = x^\circ$. Step 2 (Isosceles in $\triangle EBD$): Since $EB = DE$, we get $\angle BDE = x^\circ$. Step 3 (Exterior angle at D): $\angle AED = \angle EBD + \angle EDB = x^\circ + x^\circ = 2x^\circ$.

Step 4 (Isosceles in $\triangle ADE$): Since $AD = DE$, $\angle A = 2x^\circ$. Step 5 (Angle in $\triangle DBC$): Since $BD = BC$, $\triangle DBC$ is isosceles, so $\angle C = \angle BDC$. From the figure, $\angle BDC = 3x^\circ$. Step 6 (Isosceles in $\triangle ABC$): Since $AB = AC$, $\angle ABC = \angle C = 3x^\circ$. Step 7 (Triangle angle sum): $\angle A + \angle ABC + \angle C = 180^\circ \Rightarrow 2x + 3x + 3x = 180^\circ$. Step 8 (Solve): $8x = 180^\circ \Rightarrow x = 22.5^\circ$. Step 9 (Find $\angle A$): $\angle A = 2x = 45^\circ$.

Question: As shown in the figure, in triangle ABC, ED is the perpendicular bisector of AB , $\angle EBC = 24^\circ$, and $\angle C = 72^\circ$. Find the measure of $\angle A$.

Response: Step 1 (Triangle angle sum): In $\triangle BEC$, $\angle EBC + \angle BEC + \angle C = 180^\circ$.

Step 2 (Find $\angle BEC$): $24^\circ + \angle BEC + 72^\circ = 180^\circ \Rightarrow \angle BEC = 84^\circ$.

Step 3 (Perpendicular bisector property): ED is the perpendicular bisector of AB , so $EA = EB$.

Step 4 (Isosceles triangle AEB): Since $EA = EB$, $\triangle AEB$ is isosceles, so $\angle A = \angle ABE$.

Step 5 (Exterior angle relation): From the figure, $\angle BEC = \angle A + \angle ABE$.

Step 6 (Substitute equal angles): $\angle BEC = 2\angle A$. Given $\angle BEC = 84^\circ$, we get $2\angle A = 84^\circ$. $\angle A = 42^\circ$.

Figure 15: Qualitative comparison of CWR retrieval and reasoning performance under different retrieval weights.

1188

1189

1190

1191

1192

1193

1194

1195

1196

1197

1198

1199

1200

1201

1202

1203

1204

1205

1206

1207

1208

1209

1210

1211

1212

1213

1214

1215

1216

1217

1218

1219

1220

1221

1222

1223

1224

1225

1226

1227

1228

1229

1230

1231

1232

1233

1234

1235

1236

1237

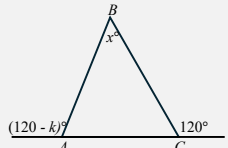
1238

1239

1240

1241

Problem



Question: In the figure above, side AC of triangle ABC is on line l . What is x in terms of k ?

Choices: (A) $60 - k$ (B) k (C) $60 + k$ (D) $120 - k$ (E) $120 - 2k$

Ground Truth: A

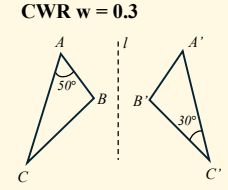
Retrieval-Specific CoT: Given information: Triangle ABC with vertices A, B, and C. Side AC is on line l . Angle at vertex C is 120° . Angle at vertex B is x° . Angle at vertex A is $(120^\circ - k)$ degrees. Angle at vertex C is $(120^\circ + k)$ degrees.

Unknowns: The value of x in terms of k .

Relevant mathematical theorems: The sum of the angles in a triangle is 180° .

Step-by-step reasoning: The sum of the angles in triangle ABC is 180° . Therefore, $x + (120^\circ - k) + (120^\circ + k) = 180^\circ$. Simplifying the equation: $x + 240^\circ = 180^\circ$. Subtracting 240° from both sides: $x = 180^\circ - 240^\circ$. Combining like terms: $x + 240^\circ = 180^\circ$. Simplifying: $x = -60^\circ$.

CWR w = 0.3



Question: As shown in the figure, $\triangle ABC$ and $\triangle A'B'C'$ are symmetric about the line l . The measure of $\angle B$ is _____.

Response: Step 1 (Symmetry Property): According to the problem, $\triangle ABC$ and $\triangle A'B'C'$ are symmetric with respect to line l , so $\angle C = \angle C' = 30^\circ$.

Step 2 (Triangle Angle Sum Theorem): The sum of the interior angles of a triangle is 180° , hence $\angle A + \angle B + \angle C = 180^\circ$.

Step 3 (Substitute Known Angles): $\angle A = 50^\circ$, $\angle C = 30^\circ$.

Step 4 (Calculate $\angle B$): $\angle B = 180^\circ - \angle A - \angle C = 180^\circ - 50^\circ - 30^\circ$.

Step 5 (Calculation Result): $\angle B = 100^\circ$.

Question: Given: As shown in the figure, $\triangle ABC \cong \triangle A'B'C'$, with $\angle A = 36^\circ$ and $\angle C' = 24^\circ$. Find: The measure of $\angle B$.

Response: Step 1 (Congruent triangles definition): From $\triangle ABC \cong \triangle A'B'C'$, we know that corresponding angles are equal: $\angle A \leftrightarrow \angle A'$, $\angle B \leftrightarrow \angle B'$, $\angle C \leftrightarrow \angle C'$.

Step 2 (Use given angle in congruent triangle): Since $\angle C' = 24^\circ$ and $\angle C$ corresponds to $\angle C'$, we have $\angle C = 24^\circ$.

Step 3 (Use given angle in original triangle): We are given $\angle A = 36^\circ$.

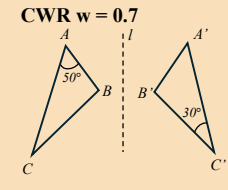
Step 4 (Triangle angle sum theorem): In any triangle, the sum of the interior angles is 180° : $\angle A + \angle B + \angle C = 180^\circ$.

Step 5 (Substitute known values): Substitute $\angle A = 36^\circ$ and $\angle C = 24^\circ$: $36^\circ + \angle B + 24^\circ = 180^\circ$.

Step 6 (Combine like terms): $\angle B + 60^\circ = 180^\circ$.

Step 7 (Solve for $\angle B$): $\angle B = 180^\circ - 60^\circ = 120^\circ$.

CWR w = 0.7



Question: As shown in the figure, $\triangle ABC$ and $\triangle A'B'C'$ are symmetric about the line l . The measure of $\angle B$ is _____.

Response: Step 1 (Symmetry Property): According to the problem, $\triangle ABC$ and $\triangle A'B'C'$ are symmetric with respect to line l , so $\angle C = \angle C' = 30^\circ$.

Step 2 (Triangle Angle Sum Theorem): The sum of the interior angles of a triangle is 180° , hence $\angle A + \angle B + \angle C = 180^\circ$.

Step 3 (Substitute Known Angles): $\angle A = 50^\circ$, $\angle C = 30^\circ$.

Step 4 (Calculate $\angle B$): $\angle B = 180^\circ - \angle A - \angle C = 180^\circ - 50^\circ - 30^\circ$.

Step 5 (Calculation Result): $\angle B = 100^\circ$.

Question: As shown in the figure, $\triangle ABC \cong \triangle DEF$. Based on the information provided in the figure, write out $x =$ _____.

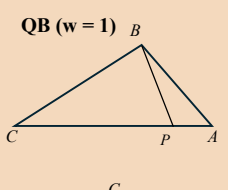
Response: Step 1 (Triangle angle sum theorem): $\angle A = 180^\circ - 50^\circ - 60^\circ$.

Step 2 (Angle calculation): $\angle A = 70^\circ$.

Step 3 (Congruent triangles corresponding sides): Since $\triangle ABC \cong \triangle DEF$, the corresponding sides are equal, so $EF = BC$.

Step 4 (Substitute side length): Given $EF = 20$, thus $x = 20$.

QB (w = 1)



Question: As shown in the image, point P is on the side AC of triangle $\triangle ABC$. Please add a condition such that $\triangle ABP$ is similar to $\triangle ACB$. This condition can be _____.

Response: Step 1 (Criteria for similar triangles): In $\triangle ABP$ and $\triangle ACB$, $\angle A$ is the common angle of the two triangles.

Step 2 (Add condition): We need one more pair of corresponding angles to be equal for the triangles to be similar, that is $\angle ABP = \angle C$.

Question: As shown in the figure, x is the length of one side of triangle ABC . The range of values for x is _____.

Response: Step 1 (Triangle Inequality Theorem): According to the triangle inequality theorem, the sum of two sides must be greater than the third side, i.e., $2 + 3 > x$. Step 2 (Calculate the sum of two sides): $2 + 3 = 5$.

Step 3 (First part conclusion): So, $x < 5$.

Step 4 (Triangle Inequality Theorem): Moreover, the difference between two sides must be less than the third side, i.e., $3 - 2 < x$.

Step 5 (Calculate the difference between two sides): $3 - 2 = 1$.

Step 6 (Second part conclusion): So, $x > 1$.

Step 7 (Combine both conclusions): Therefore, the range of x is $1 < x < 5$.

Figure 16: Qualitative comparison of CWR retrieval and reasoning performance under different retrieval weights.